



The psyllid genus *Triozidus* Li, 1994 stat. rev., *sensu novo* (Hemiptera: Psylloidea: Triozidae) in East Asia is redefined with the addition of two new species from Taiwan inducing galls on the leaflet petiolules of *Eleutherococcus trifolius* (Araliaceae)



YI-CHANG LIAO^{1,2}, HIROMITSU INOUE³ & DIANA M. PERCY^{4*}

¹Department of Entomology, University of California, Riverside, USA.



²Back to the Wild Insect Ecosurvey CO., LTD., Taichung, Taiwan.

 yeliaopsyllids@gmail.com;  <https://orcid.org/0000-0002-1595-0098>

³Institute for Plant Protection, National Agriculture and Food Research Organization, Higashihiroshima, Japan.

 hiinoue@affrc.go.jp;  <https://orcid.org/0000-0001-8197-1033>

⁴Department of Botany and Biodiversity Research Centre, University of British Columbia, Vancouver, V6T 1Z4, BC, Canada.

 diana.percy@ubc.ca;  <https://orcid.org/0000-0002-0468-2892>

*Corresponding author

Abstract

The genus *Triozidus* Li, 1994 stat. rev., *sensu novo* has a complex history. Here we redefine the genus as a natural group with two new species from Taiwan, *Triozidus burckhardti* Liao & Percy **sp. nov.** from the southernmost peninsula, and *Triozidus yangorum* Liao & Percy **sp. nov.** from the central and northern mountain region. In addition, we redescribe the type species, *Triozidus stackelbergi* (Loginova, 1967) **comb. nov.** and *Triozidus ukogi* (Shinji, 1940) **comb. nov.**, and we propose new combinations for a further two species as follows: *Triozidus ceratophorus* (Li, 2005) **comb. nov.** and *Triozidus eleutherococci* (Konovalova, 1980) **comb. nov.**; all new combinations except the latter are transferred from *Heterotrioza* Dobreanu & Manolache, and *T. eleutherococci* from *Trioza* Foerster. All but one *Triozidus* species with confirmed host plants are known to produce enclosed galls on *Eleutherococcus* (Araliaceae): *Triozidus stackelbergi* produces round galls on the leaf surface of *Eleutherococcus sessiliflorus* or more variably on leaf petioles, flowers, fruits and twigs of *E. divaricatus*; *T. ukogi* produces spindle-shaped galls on the leaf petioles or petiolules of *E. spinosus*; and *T. yangorum* produces round galls on the petiolules of the compound leaves or leaf bases of *Eleutherococcus trifolius*; *T. burckhardti* appears to share the same host plant and similar galling biology as *T. yangorum*. The description of *T. yangorum* and redescrptions of *T. stackelbergi* and *T. ukogi* are based on adults and immatures, and the immatures of *T. stackelbergi* and *T. ukogi* are described for the first time. Additionally, we provide new host and distribution records for *T. stackelbergi* in Japan. We provide identification keys for both adults and immatures, DNA barcode data for four of the six species, and an annotated mitochondrial genome for *T. yangorum*.

Key words: Asia, gall biology, jumping plant lice, Sternorrhyncha, systematics, taxonomy

Introduction

Psyllids, or jumping plant lice, (Hemiptera: Psylloidea) are phytophagous insects, ranging from 1–10 mm body length. The superfamily comprises approximately 4,000 species in over 200 genera worldwide (Li 2011; Burckhardt & Ouvrard 2012; Burckhardt *et al.* 2021; Ouvrard 2024). Psyllids feed on plant-sap and are closely associated with their host plants, often exhibiting a high level of host specificity, especially during the immature stages (Hodkinson 1974). Generally, closely related psyllid species tend to develop on closely related plant species (Burckhardt & Basset 2000; Percy *et al.* 2004). Therefore, psyllids represent an ideal model for testing hypothesis of co-evolution and co-diversification between insects and plants (Hodkinson 2009; Hollis 1987; Hollis & Broomfield 1989; Ouvrard *et al.* 2015; Percy 2003; Percy 2017; Percy *et al.* 2004).

About one fourth of psyllid species are gall inducers, and these taxa are found particularly in the families Triozidae and Calophyidae, as well as in the subfamily Phacopteroinae (Burckhardt 2005; Malenovský *et al.* 2007; Yang & Raman 2007). The most common gall type is undefined leaf distortions and open pit-galls on leaf surfaces, while enclosed galls are less common (Hodkinson 2009). Psyllid gall inducers usually show a high degree of specificity with respect to the gall formation site, shape, and host plant species (Burckhardt 2005; Hodkinson 1984).

The most important host plant families for Psylloidea are Fabaceae, Asteraceae and Myrtaceae; but there are also many plant families that are host to just a few psyllid taxa (Ouvrard *et al.* 2015; Ouvrard 2024). One of these plant families with relatively few associated psyllids is Araliaceae; only 24 psyllid species in two families (14 in Psyllidae and 10 in Triozidae) have been recorded from 26 plant species in Araliaceae (Ouvrard 2024). The bulk of the psyllid species associated with Araliaceae are found in East Asia, while three species each occur in the Afrotropical region and New Zealand, and a single species each in Hawaii and India. All species, except those treated here, are free-living. The galling species, where the host plant is known, induce completely enclosed galls on *Eleutherococcus* spp. (Araliaceae). The plant family Araliaceae includes several important traditional Chinese medicinal plants, such as *Panax* spp., and there are several species of *Eleutherococcus* that have been used for treatment of cardiovascular and cerebrovascular diseases (Huang *et al.* 2022; Sun *et al.* 2023).

Previously, only three trioziid species, *Heterotrioza stackelbergi* (Loginova, 1967), *Heterotrioza ukogi* (Shinji, 1940) and *Trioza eleutherococci* Konovalova, 1980, were known to develop on the genus *Eleutherococcus* based on the presence of immatures (Shinji 1940; Loginova 1967; Konovalova 1980; Li 2011; Cho *et al.* 2017; Kwon & Kwon 2020). These species are congeneric with the new species described here from Taiwan. Another trioziid, *Bactericera sarahae* Kwon & Kwon, 2020, may also develop on *Eleutherococcus* in South Korea (Kwon *et al.* 2022a). The original descriptions of *H. stackelbergi* and *H. ukogi* are in Russian and Japanese respectively, and the latter did not include illustrations, which may have contributed to past misidentifications (Cho *et al.* 2017). Neither of the original descriptions treated the immatures. More recent adult descriptions are provided by Kwon & Kwon (2020). We redescribe the adults and immatures of these two species. For *T. eleutherococci* and another taxon placed in *Heterotrioza*, *H. ceratophora* Li, 2005, we did not obtain specimens for redescription and include these species in the adult key according to previous descriptions (Konovalova 1980, 1988; Li 2005, 2011). In addition to the enclosed galling biology and association with *Eleutherococcus* hosts, four of the six species treated here share a distinct aedeagus morphology. The species are readily distinguished from one another in adult and immature (known for three species) stages. We provide keys and illustrations of distinguishing characters, as well as evidence for the phylogenetic position and haplotype sequence divergence using mitochondrial sequence data.

The objectives of this study are to redefine the genus *Trioziidus* that includes two new species from Taiwan; reassign and redescribe congeneric taxa; clarify the differences between the species; and clarify the position of the genus *Trioziidus* in the family Triozidae.

Materials and methods

Psyllids were collected by sweeping with a net and directly searching on host plants. Some adults were obtained after emerging from immatures from collected gall material. Specimens were then either dry mounted or preserved in 70% or 99% ethanol. To facilitate morphological analysis some specimens were slide mounted after clearing in 10–15% potassium hydroxide and examined in glycerol or permanently slide mounted in Canada balsam. Specimens, including holotypes, are deposited in the National Chung Hsing University, Taichung, Taiwan (NCHU), and some paratypes in the National Museum of Natural Science, Taichung, Taiwan (NMNS); additional material examined is in the personal collection of DP at the University of British Columbia, Vancouver, Canada (DMPC), Naturhistorisches Museum, Basel, Switzerland (NHMB) and in the collection of HI at the National Agriculture and Food Research Organization, Japan (HIC).

Photographs of slide mounted specimens were taken with a compound microscope (Leica DM 750) equipped with a digital camera (Canon EOS 600D). The photographs were montaged using focus stacking software (Helicon Focus, Helicon Soft). The morphological terminology follows Bastin *et al.* (2023).

DNA sequences of the mitochondrial cytochrome *c* oxidase subunit I (COI) obtained from specimens of *T. stackelbergi* and *T. ukogi* sampled in Japan were generated at the National Agriculture and Food Research

Organization, Japan. Genomic DNA was extracted from the whole body of each individual using the DNeasy Blood & Tissue Kit (Qiagen, Hilden, Germany) according to the manufacturer's instructions. Polymerase chain reaction (PCR) was conducted using the primers CACF and CACR (Kuznetsova *et al.* 2012) in 50 µL volumes containing 1 µL of DNA template, 1.5 µL of each primer at 10 µM concentration, 1 unit of Tks Gflex PCR polymerase (Takara Bio, Shiga, Japan), and 25 µL of 2x PCR buffer including MgCl₂. The thermal cycling conditions were as follows: an initial denaturation stage at 94 °C for 1 min, followed by 35 cycles of denaturation at 94 °C for 30 s, annealing at 45 °C for 30 s, and an extension at 72 °C for 1 min, with a final extension at 72 °C for 10 min. The PCR products were cleaned using a NucleoSpin Gel and PCR Clean-up kit (Macherey-Nagel, Düren, Germany) and directly sequenced using an ABI3730 genetic analyzer (Applied Biosystems). Sixteen sequences of this COI fragment (714 bp) were obtained (13 of *T. stackelbergi*: 1 male, 3 females, 9 immatures and 3 of *T. ukogi*: 1 male, 2 females). Two individuals (1 male, 1 female) of *T. burckhardti* were sequenced at the University of British Columbia using primers and methods given previously (Percy *et al.* 2018; Percy & Cronk 2022) for cytochrome B (cytB) and a different COI fragment (850 bp). Two individuals (1 male, 1 immature) of *T. yangorum* were sequenced for a previous study (Percy *et al.* 2018). Each species was sampled from a single population: *T. yangorum* from Sitou Forest (Taiwan), *T. burckhardti* from Hengchun peninsula (Taiwan), *T. stackelbergi* from Nagano, Honshu (Japan), and *T. ukogi* from Tochigi, Honshu (Japan). Interspecific and intraspecific genetic distances for the three *Triozidus* species were calculated from the COI data using neighbour-joining (NJ) with uncorrected p-distance in PAUP* (Swofford 2003).

We used two different phylogenetic analyses to assess the placement within Triozidae and monophyly of *Triozidus sensu novo*. The first employed the mitogenome data from Percy *et al.* (2018) to implement a maximum likelihood (ML) backbone constraint analysis that allows the placement of short DNA sequences within a broader phylogenetic framework run with RAxML v8.2.12 (Stamatakis 2014) on the CIPRES Science Gateway (Miller *et al.* 2010). The constraint tree used was the total evidence tree obtained from the mitogenome data in Percy *et al.* (2018), which already included *T. yangorum* (as “MERGE016-Genus sp”); and then *T. burckhardti*, *T. stackelbergi* and *T. ukogi* were incorporated using the COI and cytB fragment data. Data partitions were specified for codon position and RNA regions, and ML search criteria employed model GTRCAT, 1000 rapid bootstraps, and Gamma optimization of tree space. The second analysis, based on the COI data, employed a NJ distance method using uncorrected p-distances and 1000 bootstrap replicates. The NJ analysis included the three *Triozidus* taxa sequenced for the same COI fragment, in addition to two taxa from each of the three generic groups determined as suitable outgroups for *Triozidus* based on the original mitogenome analyses in Percy *et al.* (2018) (see Fig. 16).

The complete mitochondrion sequence (recovered in two partial genome assemblies) of the species of *T. yangorum* and included in the phylogenetic analysis of Percy *et al.* (2018) as “MERGE016-Genus sp” has been annotated for the current study using Geneious R8 (v.8.1.9, Biomatters Ltd., Kearse *et al.* 2012). The annotated mitochondrial genome and all partial gene sequences are available on Genbank.

Taxonomy

Family TRIOZIDAE Löw, 1879

Genus *Triozidus* Li, 1994 stat. rev.

Triozidus Li, 1994. Type species: *Triozidus acanthopanaicis* Li, 1994: 85, by original designation.

Lunatrioza Kwon, Suh & Kwon, 2022. Type-species: *Triozia stackelbergi* Loginova, 1967: 345, by original designation; *nomen nudum* [conference poster, not a published work in the sense of the International Code of Zoological Nomenclature], **syn. nov.**

Adult colour and structure. General body colour yellow-brown to dark brown, with light to mid-brown on areas of dorsum and legs, and darker brown to black on some or all of antennal flagellum, head and pronotum, and abdominal tergites. Forewing membrane clear or yellowish, with or without distinct dark patch around clavus. Medium to large bodied, 3.5–6.0 mm (including wings). Head narrower to slightly wider than thorax, inclined at about 45–50° from longitudinal body axis (in lateral view). Head with well developed, medium-long genal processes, vertex trapezoidal, moderately concave medially at posterior margin, lateral ocelli on small tubercles, medial epicranial suture distinct.

Clypeus narrowly rounded ventrally, distal proboscis segment short. Antennae medium long, slender, 10-segmented, segment 3 longest, a single rhinarium subapically on segments 4, 6, 8 and 9. Thorax weakly to moderately arched. Pronotum deflexed from mesothorax at a 45° angle. Legs moderately short and robust, tibia longer than femur; hind leg with meracanthus well developed, horn-shaped, more or less straight, acute at apex; metatibia length equal to or longer than head width, with a single or cluster of small spines basally, inflated apically and bearing 3 (1+2) sclerotized apical spurs (not stalked) and a row of unsclerotized bristles; metabasitarsus without apical spurs, slightly longer than apical metatarsus. Forewing relatively large, length approximately 1.2–1.5 x body length, broadest in the middle or distal to the middle, with trifurcation of veins R+M+Cu strict; membrane lacking surface spinules except occasional small area with spinules at base of cell cu₂, a narrow cluster of marginal radular spines present at wing margin, more or less centrally positioned in cells m₂ and cu₁, and in the posterior half of cell m₁; size of cell m₁ subequal to, or notably larger than, cell cu₁; vein Rs either long and sinuous or medium short and evenly curving to fore margin; forewing apex subacute to acute. Hindwing medium-short, length less than 2/3 forewing length. Male terminalia with subgenital plate globose, posterior margin more or less rounded or more angular (in lateral view); proctiger short with slight to moderate posterior lobe medially, length subequal or shorter than paramere; paramere simple (in lateral profile), more or less parallel sided, either straight, moderately sinuous or with incision medially on anterior surface, tapering to blunt or pointed apex; distal aedeagus segment either distinctly angled or arched with a bipartite projection medially consisting of either thumb-like or semicircular projections, or less typically more or less straight and lacking such projections, apex inflated and developed into a shallow or widely curving hook. Female terminalia short, length approximately subequal to head width, proctiger slightly longer than subgenital plate, anal ring large and consisting of a single row of pores. Ovipositor dorsal valvulae relatively small and cuneate, ventral valvulae with one or a few shallow serrations.

Immature colour and structure. *Fifth instar immature.* Coloration. General body colour yellowish-brown to dark brown, with light to mid-brown areas on dorsum and legs, and darker brown to black on some sclerites and terminal antennal segments. Body shape in dorsal view elongate-oval with wing pads protruding and humeral lobes developed; sclerites present dorsally and ventrally. Body surface covered with medium dense simple setae or sectasetae. Antenna weakly curved, 8-segmented; scape, pedicel and segment 3 thicker than remaining flagellum; with a single subapical rhinarium on each of segments 4 and 6, and two on segment 8. Legs moderately long, femur shorter than tibiotarsus; tarsi with only one fully developed claw (outer), tarsal arolium longer than claws, triangular with a medial cleft, with short unguitactor, lacking pedicel. Humeral lobe of forewing pad relatively short, reaching hind margin of eye. Caudal plate broadly rounded posteriorly. Circumanal ring in ventral position, relatively wide and short; outer ring mostly composed of a single row of elongate pores, or with convolutions and intermittent multi-pore sections.

Egg. Only known for *T. stackelbergi*. Oblong-ovoid with a short, laterally positioned pedicel sub-basally on underside and short tail (illustrated in Loginova 1967).

Host plant. *Eleutherococcus* spp. (Araliaceae).

Biology. All species for which biology is known produce enclosed galls on some or all of the following host organs: leaves, twigs, male and female flowers, petioles or petiolules.

Distribution. The genus occurs in China (Li 2011), Japan (Shinji 1940, Miyatake 1996), Russia (Loginova 1967, Konovalova 1988), South Korea (Cho *et al.* 2017, Kwon & Kwon 2020), and Taiwan (this study).

Comment. The genus includes four described nominal species and two new species. Kwon & Kwon (2020) synonymised *Triozidus acanthopanaicis* Li, 1994, the type species of *Triozidus*, with *Heterotrioza stackelbergi*. Species of *Triozidus sensu novo* have been variously referred to *Heterotrioza* Dobreanu & Manolache, *Heterotrioza* (*Dyspersa*) Klimaszewski, *Trioza* or *Triozidus* (Klimaszewski 1973; Li 2011; Kwon & Kwon 2020; Cho *et al.* 2022). Loginova (1967) discussed morphological differences between *T. ukogi* and *T. stackelbergi*, and Cho *et al.* (2017) pointed out that the latter has been misidentified repeatedly in the literature from Korea as either *Trioza ukogi*, *Heterotrioza* (*Dyspersa*) *ukogi* or *Heterotrioza ukogi*.

Unusual features of the genus typically, but not exclusively, include the bipartite projection on the shaft of the apical aedeagus segment (i.e., not on the apex as in *Heterotrioza*), and the immatures with uneven or asymmetrical development of tarsal claws; interestingly, it seems that the undeveloped claw becomes increasingly vestigial in later instars. Many trioziid groups are known to be relatively morphologically homogeneous resulting in peripatetic taxonomic histories, and this is especially the case with taxa formerly placed within the catch-all genus *Trioza*. These challenges have increased the reliance on molecular data, and the reciprocal illumination these data offer, to help

resolve morphologically challenging groups. Nevertheless, *Triozidus* has a number of morphological characters that collectively serve to help distinguish it from related groups. In particular, the large size of the forewing relative to body size is more exaggerated than in related genera (e.g., *Dyspersa*, *Heterotrioza*, *Lauritrioza* Conci & Tamanini, *Trioza* s.s.), the forewing cell m_1 is always larger than cu_1 (usually markedly so), the transition from vertex to genal cones is not as distinctly stepped, and the apex of the metatibia is more expanded. These, together with the biology and host plants in *Eleutherococcus*, and the immature vestigial claw, define *Triozidus*. Relationships with other *Trioza sensu lato* taxa and other genera in Group B (as shown in Fig. 16), are still in flux taxonomically as these groups become more well defined, but the same assemblage of characters given above, together with the molecular data, provides the best diagnosis.

Key to adults of *Triozidus*

1. Forewing with Rs vein long and sinuous (terminating distal to a line drawn through termination of vein Cu_{1a} and bifurcation of vein M); cell cu_1 higher resulting in cell m_1 not being markedly larger than cell cu_1 (Fig. 9B); on *Eleutherococcus spinosus* (or other *Eleutherococcus* spp. where alien) *Triozidus ukogi* (Shinji, 1940) **comb. nov.**
- Forewing with Rs short and more or less evenly curving to the fore margin (terminating at or proximal to a line drawn through termination of vein Cu_{1a} and bifurcation of vein M); cell cu_1 lower and cell m_1 markedly larger than cell cu_1 (Figs 2E, 5C, 13D); on other *Eleutherococcus* species (where host plant is known) 2
2. Antennae shorter than 1.5 x head width; apex of paramere (in lateral profile) tapering to a slender, anteriorly directed point (Fig. 16) *Triozidus ceratophorus* (Li, 2005) **comb. nov.**
- Antennae longer than 1.5 x head width; apex of paramere (in lateral profile) more or less blunt and directed inward or posteriorly (Figs 3B, 6B, 14B, 16) 3
3. Body including forewing shorter than 4.5 mm; distal aedeagus segment lacking medial projections (Figs 3C, 16) 4
- Body including forewing longer than 4.5 mm; distal aedeagus segment with distinct medial projections (Figs 6C, 14C, 16) .. 5
4. Head and antennae entirely black (Fig. 1A); paramere (in lateral profile) with distinct angular incision medially on anterior surface, apex rounded (Figs 3A, 3B, 16) *Triozidus burckhardti* **sp. nov.**
- Head mostly yellow-brown to orange-brown with probably only terminal antennal segments black; paramere (in lateral profile) without angular medial incision but with slight incision near the base on anterior surface, apex elongate and extended rearward (Fig. 16) *Triozidus eleutherococci* (Konovalova, 1980) **comb. nov.**
5. Genal processes shorter (length just over half vertex length, < 0.3 head width) and more blunt apically (Fig. 13A); forewing with distinct dark marginal patch around clavus, but without a small dark spot at trifurcation of R+M+Cu (Fig. 13D); forewing broader (ratio length:width < 2.6), widest distal to middle, length approximately 2 x Rs vein length (Fig. 13D); paramere broader (in lateral profile) (Figs 14A, 14B, 16); distal aedeagus segment with medial projections narrow and thumb-like (Figs 14C, 16); female terminalia shorter (length of proctiger less than head width and < 3 x anal ring length) (Fig. 14D); on *Eleutherococcus trifolius* *Triozidus yangorum* **sp. nov.**
- Genal processes longer (length approximately equal to vertex length, > 0.3 x head width) and more acute apically (Fig. 5A); forewing without distinct dark marginal patch around clavus, but with a small dark spot at trifurcation of R+M+Cu (in Japanese and South Korean material, see Fig. 5C, but possibly absent in eastern Russia material); forewing narrower (ratio length:width > 2.6), widest in middle, length approximately 2.5 x Rs vein length; paramere narrower (in lateral profile) (Figs 6A, 6B, 16); distal aedeagus segment with medial projections semi-circular (Figs 6C, 16); female terminalia longer (length of proctiger greater than head width and > 3 x anal ring length) (Fig. 6D); on *Eleutherococcus sessiliflorus* and *E. divaricatus* (or other *Eleutherococcus* spp. where introduced) *Triozidus stackelbergi* (Loginova, 1967) **comb. nov.**

Key to 5th instar immatures of *Triozidus*

(known for three species)

1. Body covered in narrow truncate setae (Fig. 7C) *Triozidus stackelbergi* (Loginova, 1967) **comb. nov.**
- Body covered in long simple setae (Figs 11C, 15C) 2
2. Circumanal ring heart-shaped (medial constriction mainly from anterior), outer ring composed of a mix of elongate and irregular shaped pores (Fig. 15D) *Triozidus yangorum* **sp. nov.**
- Circumanal ring peanut-shaped (with antero-posterior medial constriction), outer ring composed of a single narrow row of elongate pores (Fig. 11D) *Triozidus ukogi* (Shinji, 1940) **comb. nov.**

Note on species descriptions. The species descriptions below provide details of species specific characteristics not supplied in the generic description above.

***Triozidus burckhardti* Liao & Percy sp. nov.**

(Figs 1A–B, 2, 3)

Type material. **Holotype:** TAIWAN • ♂; Pingtung Co., Manzhou, Changle; 22°04'53.9"N, 120°50'09.5"E; 29 Jan 2024; Y. C. Liao leg.; *Eleutherococcus trifolius*; NCHU, dry mounted. **Paratypes:** TAIWAN • 1♂, 1♀; same data as for holotype, but in ethanol and slide mounted. 1♂, 2♀; same data as for holotype, but DMPC, in ethanol. 1♂, 1♀; same data as for holotype, but NHMB, in ethanol. 3♀; same data as for holotype, but 26 Mar 2020.

Description. *Adult* (Figs 1A, 2, 3). Coloration. Body color yellowish brown with entire head, compound eyes and antennae black (Fig. 1A). Abdominal tergites blackish brown. Legs yellow. Forewing pale yellow, transparent, slightly darker brown around clavus (Fig. 2E). Hindwing transparent.

Structure. Body median-sized, length from anterior head margin to tip of folded forewing 3.6–3.8 mm, female generally larger. Head (Fig. 2A) slightly narrower than thorax. Vertex width 1.7–1.8 x length, minutely pubescent. Genal processes prominent, length along mid-line 0.7–0.8 x vertex length, divergent, conical, acute at apex, covered in short hair. Antenna (Fig. 2B) length 1.8–2.0 x head width, antennal segment 3 approximately double length of segment 4, relative length of flagellar segments as 1.0: 0.5: 0.3: 0.4: 0.3: 0.3: 0.2: 0.2; two unequal terminal setae: longer seta 0.7 x, and shorter seta 0.3 x segment 10 length. Thorax moderately arched dorsally, minutely pubescent. Hind leg (Fig. 2C) metatibia length 1.0–1.1 x head width. Forewing moderately broad (Fig. 2E), length 5.8–5.9 x head width, and 2.9–3.0 x width, widest slightly distal to the middle; wing apex acute; vein Rs moderately long, gradually curved to fore margin; vein M evenly curved with bifurcation posterior to line connecting apices of veins Rs and Cu_{1a}; cell m₁ larger than cell cu₁; vein Cu_{1a} evenly curved, vein Cu_{1b} straight; veins minutely pubescent. Hindwing (Fig. 2D) 0.6 x as long and 0.5 x as wide as forewing.

Male terminalia (Figs 3A–C). Proctiger short, with moderate posterior lobes reaching maximum extension in the basal half (Fig. 3A). Subgenital plate subglobular, with medium long setae laterally and ventrally; posterior dorsal margin slightly convex. Paramere (Fig. 3B) slightly longer than proctiger; in profile angulate at base, with a deep incision anteriorly in the basal half, before narrowing to apex which is acute and directed inward; inner face and surface beset with median-long setae. Distal aedeagus segment (Fig. 3C) about as long as paramere (Figs 3A, 16), straight medially without projection, apical portion largely inflated into a hook with acute apex; sclerotized end tube of ductus ejaculatorius short, slightly sinuous. **Female terminalia** (Fig. 3D) cuneate, short; proctiger dorsal margin slightly sinuate with medial depression and acute apex, only slightly longer than subgenital plate, with long setae in the apical half, anal ring length approximately one third proctiger length, consisting of a single row of pores. Subgenital plate, in profile, triangular, apex acute, beset with long hairs laterally and ventrally. Ovipositor dorsal valvulae cuneate, ventral valvulae straight with several shallow serrations apically.

Measurements in mm (1 male, 1 female). Body length (including forewing) ♂ 3.56; ♀ 3.75. Head width ♂ 0.47; ♀ 0.52. Vertex width ♂ 0.27; ♀ 0.31. Vertex length ♂ 0.16; ♀ 0.17. Genal cone length ♂ 0.11; ♀ 0.13. Antenna length ♂ 0.93; ♀ 0.93. Metatibia length ♂ 0.50; ♀ 0.53. Forewing length ♂ 2.75; ♀ 3.0. Forewing width ♂ 0.93; ♀ 1.05. Aedeagus length ♂ 0.20. Paramere length ♂ 0.22. Proctiger length ♀ 0.62. Subgenital plate length ♀ 0.60.

Etymology. The specific name honours Dr Daniel Burckhardt for his contribution to our knowledge of the world's psyllid fauna.

Distribution. Taiwan; only found in the southernmost part (Hengchun peninsula).

Host plant. Probably *Eleutherococcus trifolius* (Araliaceae), but immature specimens are needed to confirm host and gall type.

Biology. This species apparently shares the same host plant as *T. yangorum* but the two psyllid species are allopatric, with *T. burckhardti* only found in the southernmost part of Taiwan and *T. yangorum* in central and northern Taiwan. They also appear to have a similar galling biology, galls and immatures were recorded for *T. burckhardti* but no immature specimens were preserved. Immatures (1st instar) were observed to develop within fully enclosed round galls that are positioned on the base of leaflets, or just below the leaflets on the petiolules, or on the leaf petioles. Each gall consists of a single gall chamber with usually a single immature. Galls are found individually or in aggregates of two to four galls per leaf, often with a gall on each of the three petiolules (Fig. 1B). As is the case for *T. yangorum*, *T. burckhardti* is univoltine with adults emerging in January.

Genetic resources. Adult male and female sequences of COI and cytB were identical, unique haplotypes: PQ817990 and PQ817253 (for COI and cytB respectively).

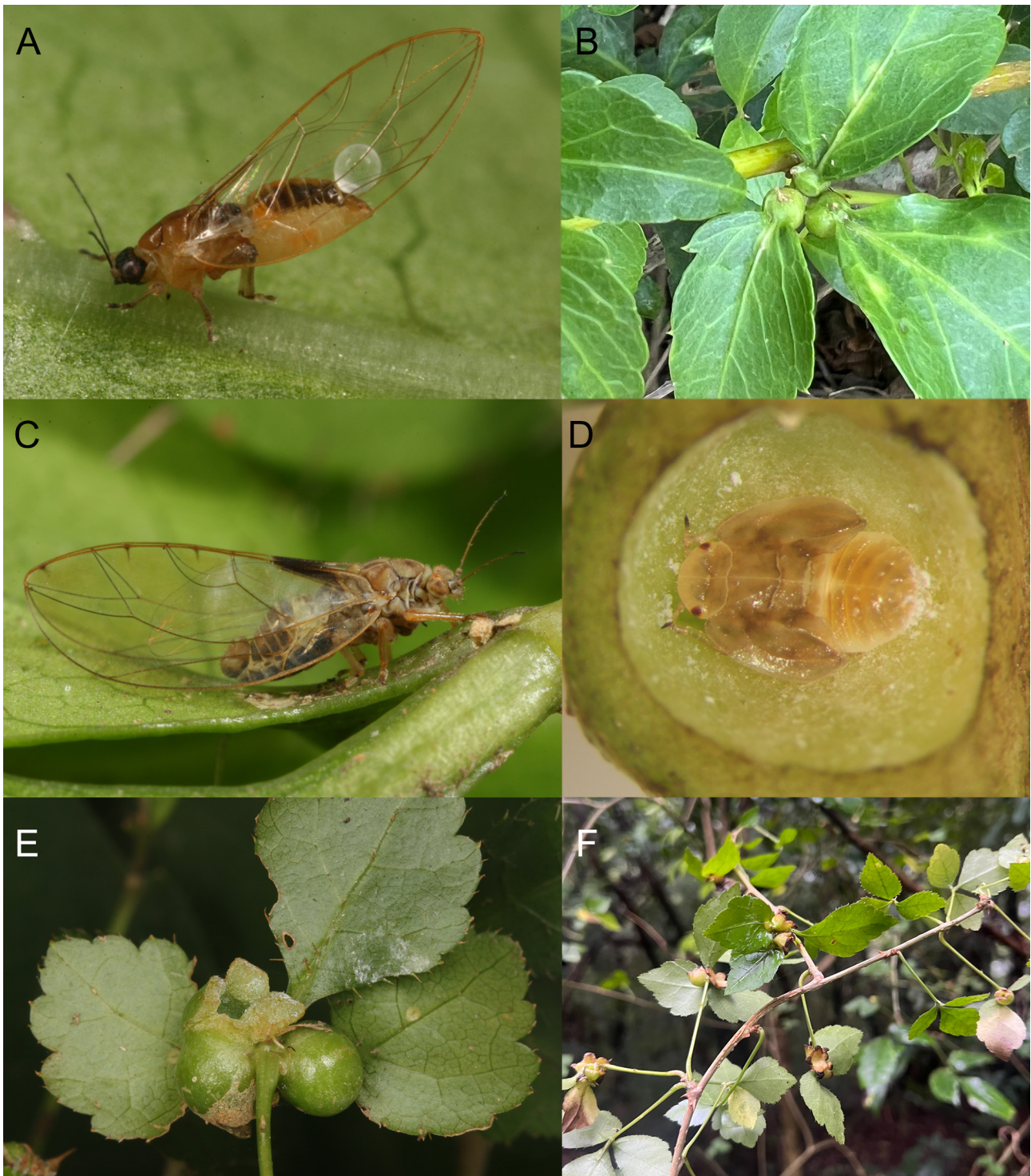


FIGURE 1. *Triozidus burckhardti* **sp. nov.** and *Triozidus yangorum* **sp. nov.** adults, immature and galls on the host plant, *Eleutherococcus trifolius*. **A**, *T. burckhardti* female; **B**, closed galls of cf. *T. burckhardti* with a single gall on each petiolule of the trifoliate leaf; **C**, *T. yangorum* male; **D**, *T. yangorum* fifth instar immature within gall chamber; **E**, close up showing three petiolule galls of *T. yangorum* on a single leaf, the upper already opened; **F**, the scandent host, *E. trifolius*, showing distribution of petiolule galls.

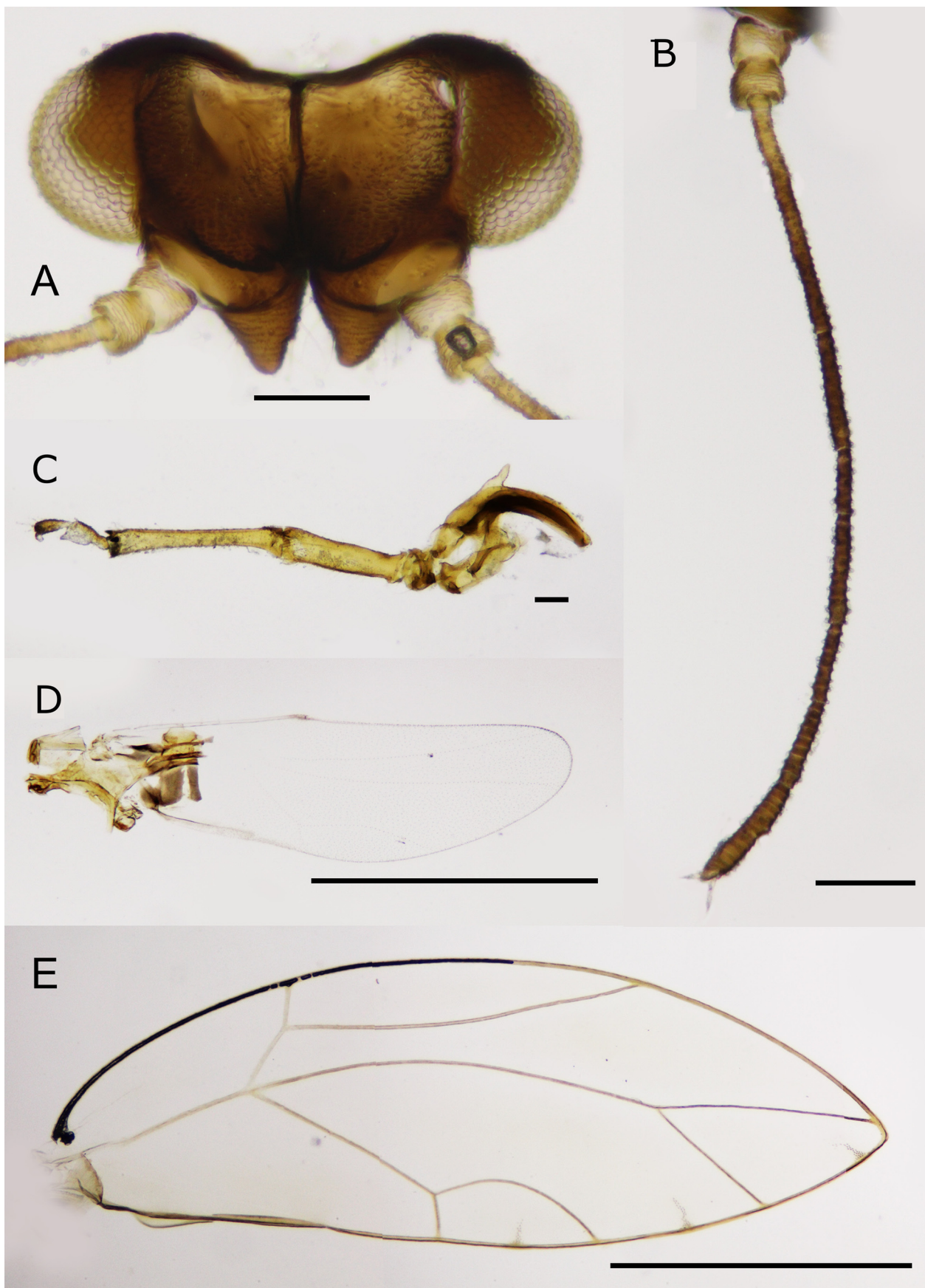


FIGURE 2. Adult *Triozidus burckhardti* **sp. nov.** **A**, head; **B**, antenna; **C**, hind leg; **D**, hindwing; **E**, forewing. Scale bars: 0.1 mm (A, B, D); 1 mm (C, E).

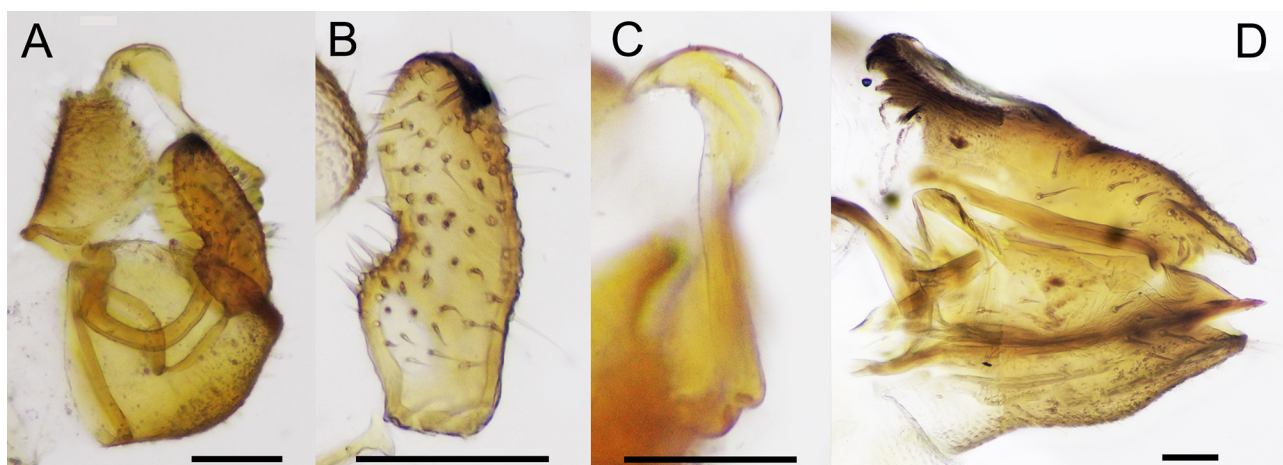


FIGURE 3. Terminalia of *Trioizidus burckhardti* sp. nov. **A**, male terminalia (lateral view); **B**, paramere (inner surface); **C**, distal segment of aedeagus; **D**, female terminalia (lateral view). Scale bars: 0.1 mm.

***Trioizidus ceratophorus* (Li, 2005) comb. nov.**

Heterotrioza ceratophora Li, 2005: 201.

Material examined. None.

Description. Adult described from a single male (Li 2005, 2011).

Host plant. Unknown.

Distribution. China (Gansu) (Li 2005, 2011).

Comment. Li's (2011) key to *Heterotrioza* separates *T. ceratophorus* and *T. stackelbergi* from other taxa that belong in *Heterotrioza* based on wing characters that highlight the much larger size of cell m_1 relative to cu_1 in the *Trioizidus* taxa. Additionally, *T. ceratophorus* possesses the medial projections on the distal aedeagus segment that is typical for *Trioizidus*, versus the terminal projections typical for *Heterotrioza*.

***Trioizidus eleutherococci* (Konovalova, 1980) comb. nov.**

Trioza eleutherococci Konovalova, 1980: 21.

Material examined. None.

Description. Adult male and female in Konovalova (1980), with additional information in the key in Konovalova (1988).

Host plant. Given as *Eleutherococcus senticosus* in Konovalova (1980) but no mention of galls.

Distribution. Russia (Primorsky Krai, Russian Far East) (Konovalova 1980, 1988).

Comment. This species, like *T. burckhardti*, lacks the medial projections on the distal aedeagus segment. The paramere shape is diagnostic with the apex extended rearward more so than in other *Trioizidus* (Fig. 16). Other distinguishing characters that also suggest this species may be most closely related to *T. burckhardti* are small size (overall body size less than 4.5 mm, forewing length less than 3.5 mm) (Fig. 16), relatively narrow forewing, and genal cones that are short and acute (Konovalova 1980, 1988).

***Trioizidus stackelbergi* (Loginova, 1967) comb. nov.**

(Figs 4–7)

Trioza stackelbergi Loginova, 1967: 345.

Heterotrioza (Dyspersa) stackelbergi: Klimaszewski (1973: 248).

Triozidus acanthopanaicis Li, 1994: 85, synonymised by Kwon & Kwon (2020: 220).

Heterotrioza acanthopanaicis: Li (2011: 1521).

Heterotrioza stackelbergi: Kwon & Kwon (2020: 220), Cho *et al.* (2022: 72).

Lunatrioza stckelbergi [sic] Kwon, Suh & Kwon, 2022: *nomen nudum* [conference poster, not a published work in the sense of the International Code of Zoological Nomenclature].

Material examined. KOREA • 4 ♂, 3 ♀; Yeong wol-gun, Jucheon-myeon, Jucheon-ri, Swimteo Park; 37°26'09.3"N, 128°29'26.9"E; 3 Oct 2014; Jin-Yeong Choi leg.; NCHU, slide mounted, glycerol and ethanol. JAPAN • 6 ♀, 1 immature; Honshu, Nagano Pref., Kitasaku-gun, Minamimaki-mura, Nobeyama; 35.93515 N, 138.46349 E, 1370 m; 16 Oct. 2018; Akihide Koguchi leg.; *Eleutherococcus divaricatus* (twig galls, flower galls); HIC, dry, slide mounted. 15 ♂, 14 ♀, 4 immatures; same data but 6. Oct. 2019; HIC, NCHU, dry, slide mounted and in ethanol. 20 ♂, 27 ♀, 18 immatures; Honshu, Nagano Pref., Kitasaku-gun, Minamimaki-mura, Itabashi; 35.97757 N, 138.47251 E, 1350 m; 6 Oct. 2019; Akihide Koguchi leg.; *Eleutherococcus divaricatus* (twig galls, flower galls); HIC, NCHU, dry, slide mounted and in ethanol.

Note. The redescription below is based on material examined from Japan and South Korea, as well as the description in Loginova (1967) of eastern Russia material and notes on Chinese specimens by Li (2011). Measurements given below are taken from the material from Japan and South Korean, with measurements, if different and where reported in Loginova (1967), shown in [].

Description. *Adult* (Figs 4A–B, 5, 6). Coloration. General body color brown (Japan and South Korean), or yellow-orange with parts brown (eastern Russia; Loginova 1967). Antennae with apical half of 1st segment and the remaining antenna dark brown (Japan and South Korean), or only terminal segment dark (eastern Russia; Loginova 1967). Compound eyes dark brown. Ocelli orange. Legs brown. Forewing veins brown, membrane transparent, with

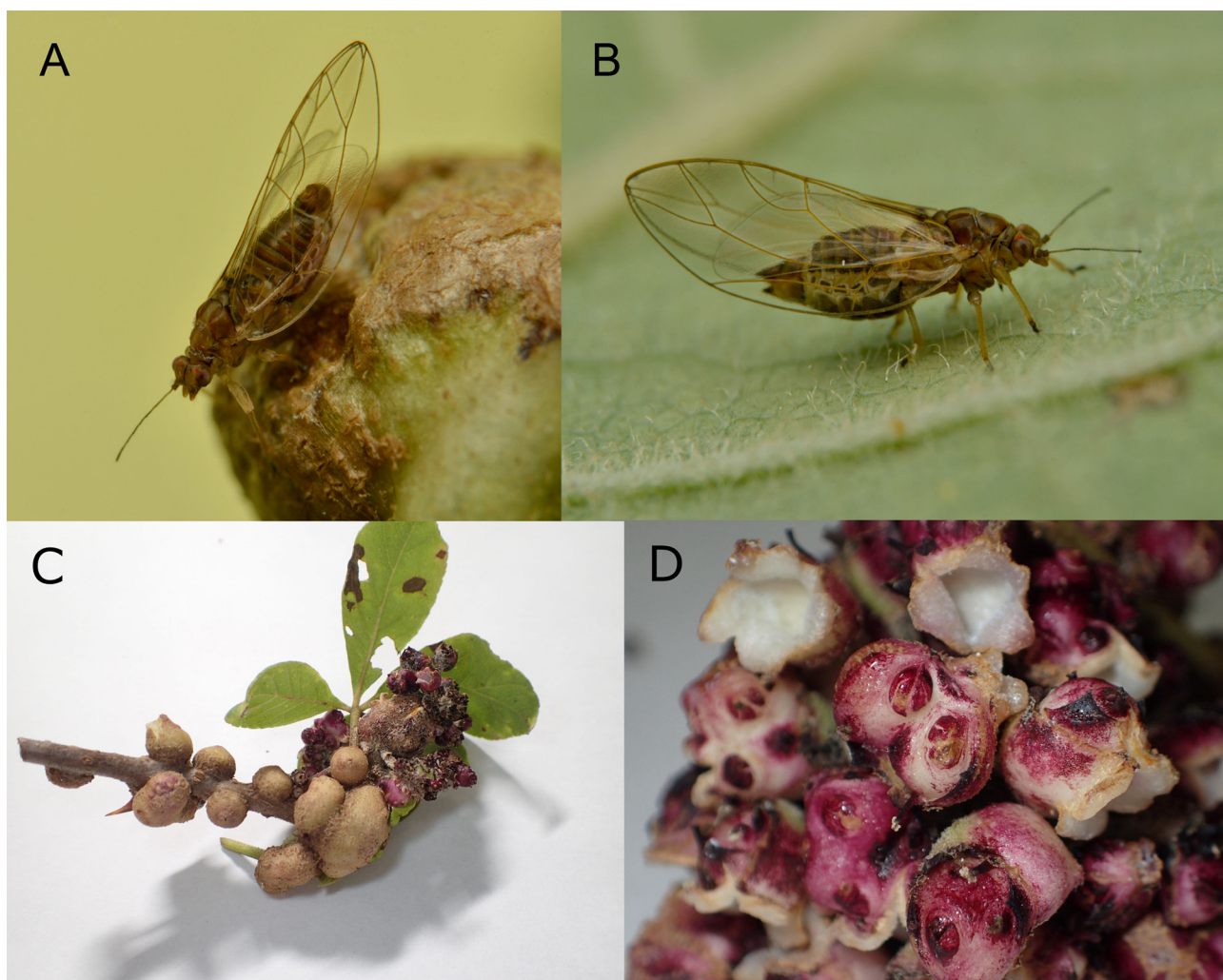


FIGURE 4. *Triozidus stackelbergi* adults and galls on *Eleutherococcus divaricatus*. **A**, male; **B**, female; **C**, twig and male flower galls on *E. divaricatus*; **D**, detail of male flower galls.

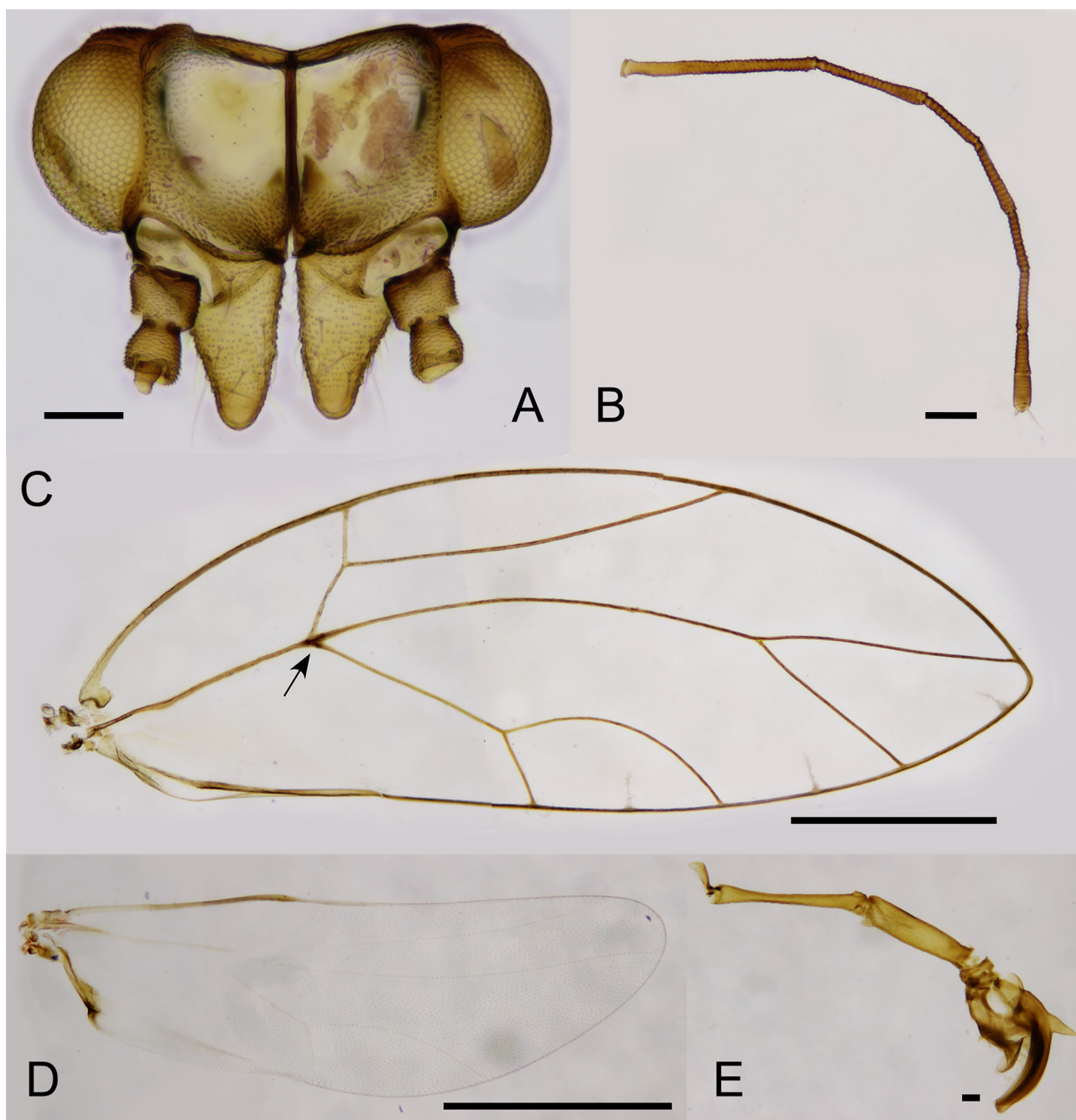


FIGURE 5. Adult *Triozidus stackelbergi* **comb. nov.** **A**, head; **B**, antenna; **C**, forewing, with small dark spot at trifurcation of R+M+Cu (arrowed); **D**, hindwing; **E**, hind leg. Scale bars: 0.1 mm (A, B, E); 1 mm (C, D).

a small dark spot at trifurcation of R+M+Cu₁ in Japanese and South Korean material, but possibly absent in eastern Russia material or omitted from Loginova's (1967) description.

Structure. Body large-sized, length from anterior head margin to tip of folded forewing 5.3–5.8 mm [4.6–5.7 mm], female generally larger; covered in short fine setae. Head (Fig. 5A) slightly narrower than thorax. Vertex width 1.4–1.5 x [1.6 x] length, minutely pubescent. Genal processes prominent, length along mid-line 0.8–1.0 x vertex length, divergent, conical, subacute at apex, with long pubescence. Antenna (Fig. 5B) length 2.0–2.1 x [1.9–2.0 x] head width, antennal segment 3 approximately 1.4 x segment 4, relative length of flagellar segments as 1.0: 0.7: 0.3: 0.4: 0.3: 0.3: 0.2: 0.2; two unequal terminal setae: longer seta 1.1 x, and short, truncate seta 0.2 x segment 10 length. Thorax weakly arched dorsally, minutely pubescent. Hind leg (Fig. 5E) metatibia length 1.2–1.3 x head width. Forewing (Fig. 5C) relatively long and narrow, length 6.0–6.6 x head width, and 2.8–2.9 x width,

widest in the middle; wing apex acute; vein Rs moderately long, gradually curved to fore margin; vein M evenly curved with bifurcation posterior to line connecting apices of veins Rs and Cu_{1a}; cell m₁ larger than cell cu₁; vein Cu_{1a} evenly curved, vein Cu_{1b} straight; veins minutely pubescent. Hindwing (Fig. 5D) 0.65 x as long and 0.5 x as wide as forewing.

Male terminalia (Fig. 6A–C). Proctiger short, with moderate posterior lobes reaching maximum extension in the basal half, covered in long setae except for basal third laterally (Fig. 6A). Subgenital plate subglobular, with medium long setae laterally and ventrally; posterior dorsal margin slightly convex. Paramere (Fig. 6B) about as long as proctiger; in profile more or less parallel sided and straight, slightly sinuous, irregularly narrowing to apex which is acute and directed inward and rearward; inner face beset with long setae, outer surface with shorter setae. Distal aedeagus segment (Fig. 6C) slightly shorter than paramere (Figs 6A, 16), curved medially with semi-circle projections, apical portion inflated, crescent-shaped, with acute apex [eastern Russian specimens have distal aedeagus segment slightly longer, less curved medially and the semi-circular projections are less extended]; sclerotized end tube of ductus ejaculatorius short, sinuous. Female terminalia (Fig. 6D) cuneate, slender; proctiger abruptly narrowing in apical fourth with acute apex, dorsal margin more or less straight, slightly longer than subgenital plate, with long setae in the apical half, anal ring length approximately one fourth proctiger length, consisting of a single row of pores. Subgenital plate, in profile, triangular, apex acute, beset with medium long hairs laterally and ventrally. Ovipositor dorsal valvulae cuneate, ventral valvulae straight with a single shallow serration.

Fifth instar immature [based on specimens from Japan] (Fig. 7). Coloration. General color brown. Forewing pad and thorax pale brown. Body (Fig. 7A) length 1.3–1.4 x width. Body surface, including margin of head, wing pads (Fig. 7C), caudal plate and legs covered with medium dense, narrow truncate sectasetae. Antenna (Fig. 7E) relative length of antennal segments 3 to 8 as 1.0: 0.5: 0.5: 0.4: 0.6: 1.4. Legs (Fig. 7B) as for generic description. Forewing pad length 2.9 x width, and 2.6 x antenna length. Caudal plate length 0.7 x width. Circumanal ring (Fig. 7D) heart-shaped (medial constriction mainly from anterior); width 0.3 x caudal plate width; outer ring mostly composed of a single row of elongate pores with a few intermittent irregular pore shapes; inner ring composed of a mixture of short and elongate pores.

Host plant. *Eleutherococcus sessiliflorus* in Russia (Loginova 1967) and South Korea (Cho *et al.* 2017), *Eleutherococcus divaricatus* in Japan (this study), and *Eleutherococcus senticosus* in China (Li 2011) and South Korea (according to Kwon & Kwon 2020).

Biology. Induces round galls on the leaf surface in South Korea (illustrated in Cho *et al.* 2017; Kwon & Kwon 2020), but in Japan produces rounded galls, sometimes at high densities, on twigs, stems and leaf petioles, as well as on male and female flowers (Fig. 4C–D). In Japan, it appears to be bivoltine, with the first generation adults emerging in early summer (June–July) and the second generation around October (A. Koguchi, personal communication).

Distribution. China (Li 2011), Eastern Russia (Loginova 1967) and South Korea (Cho *et al.* 2017, Kwon & Kwon 2020), and reported here for the first time for Japan.

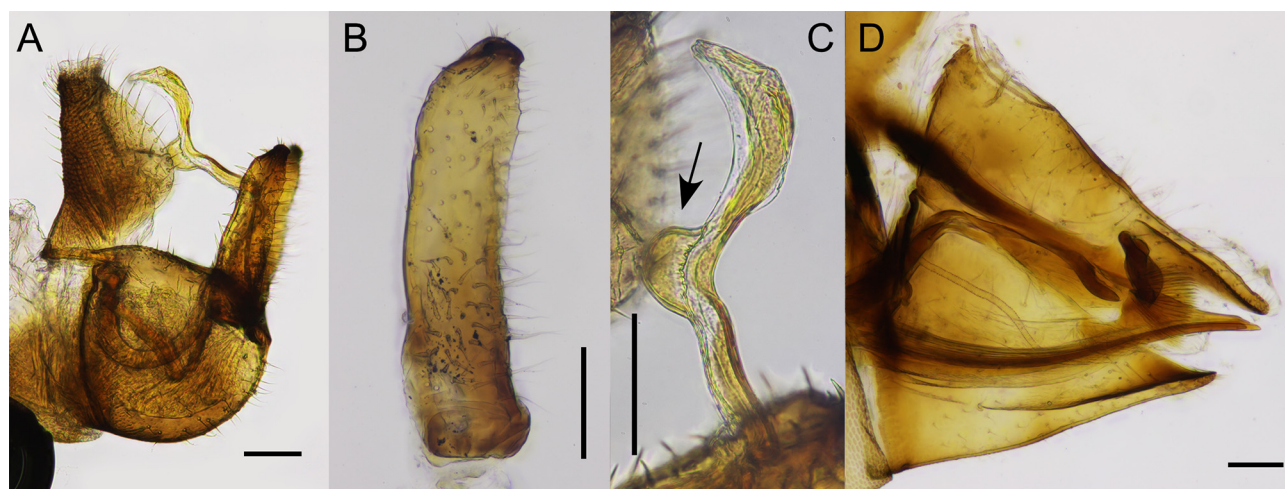


FIGURE 6. Terminalia of *Trioizidus stackelbergi* **comb. nov.** **A**, male terminalia (lateral view); **B**, paramere (inner surface); **C**, distal portion of aedeagus showing medial semicircular projections (arrowed); **D**, female terminalia (lateral view). Scale bars: 0.1 mm.

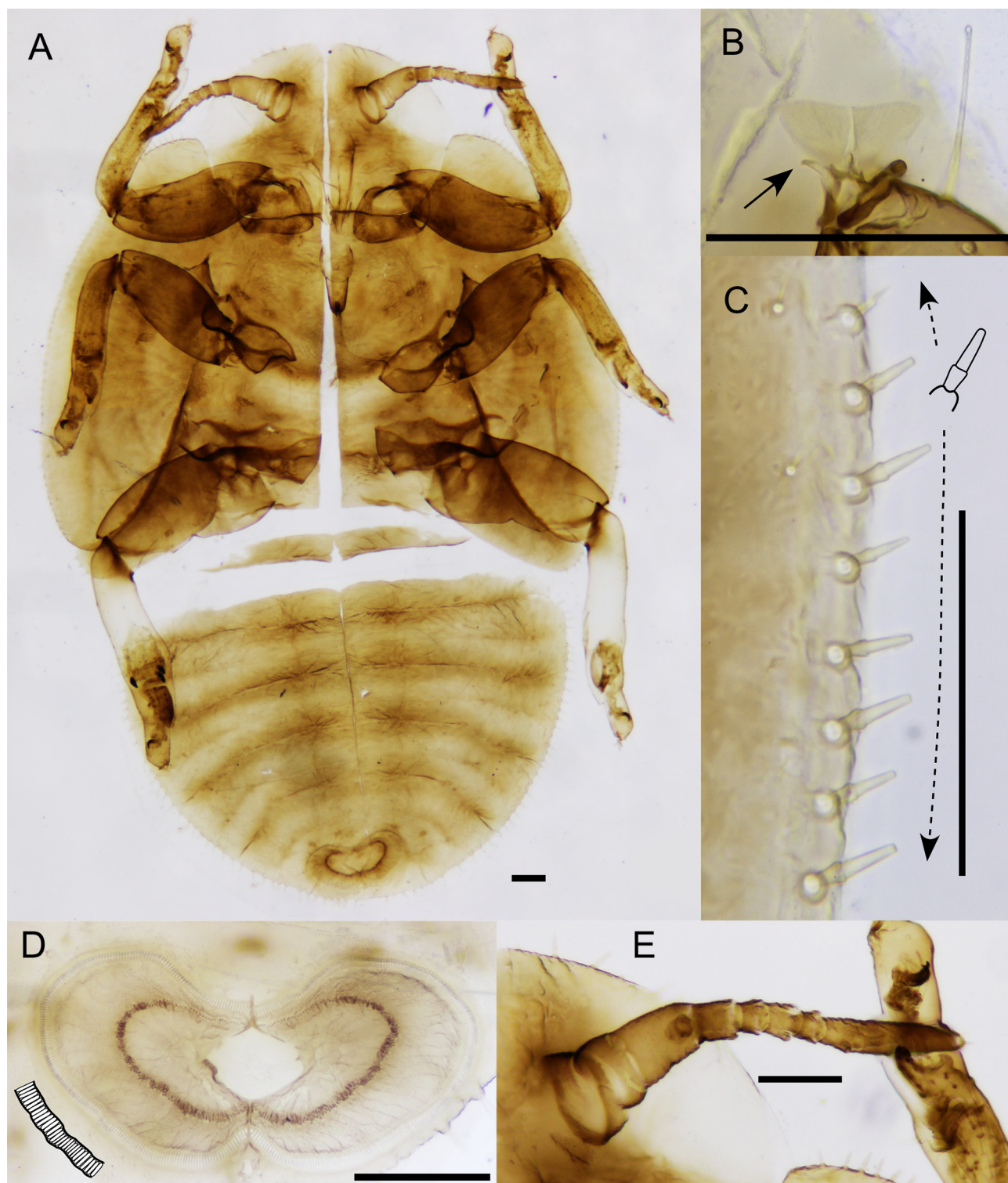


FIGURE 7. Fifth instar immature of *Triozidus stackelbergi* **comb. nov.** **A**, habitus; **B**, tarsal arolium showing asymmetric development of tarsal claws (vestigial claw arrowed); **C**, forewing pad marginal sectasetae; **D**, circumanal ring showing regular single row of pores (inset); **E**, antenna. Scale bars: 0.1 mm.

Comment. Specimens examined from Japan and South Korea conform closely to the original description and illustrations by Loginova (1967) based on material from eastern Russia. Loginova (1967) reports a slightly smaller body size (4.6–5.7 mm) compared to the Japanese and Korean material (5.3–5.8 mm), and a forewing shape that is slightly longer and narrower, with the relative size difference between cells cu_1 and m_1 more marked; Loginova

(1967) also does not mention a dark spot at trifurcation of R+M+Cu, although this may simply be omitted from her description. We also note that specimens from South Korea are marginally larger than Japanese material. Altogether, the differences equate to moderate natural variation across the species range. Kwon & Kwon (2020) list this species as a pest on medicinal *Eleutherococcus* spp. in South Korea.

Genetic resources. Adult and immature sequences of COI were identical, unique haplotype: PQ817986.

***Triozidus ukogi* (Shinji, 1940) comb. nov.**

(Figs 8–11)

Triozidus ukogi Shinji, 1940: 66.

Heterotriozidus (Dyspersa) ukogi: Klimaszewski (1973: 248).

Heterotriozidus ukogi: Kwon & Kwon (2020: 221); Cho *et al.* (2022: 72).

Lunatriozidus ukogi Kwon, Suh & Kwon, 2022: *nomen nudum* [conference poster, not a published work in the sense of the International Code of Zoological Nomenclature].

Material examined. JAPAN • 6♂ 7♀; Honshu, Tochigi Pref., Utsunomiya City, Kamikuwajima-machi; 36.525 N, 139.949 E, 92 m; 28 Oct 2014; Rikio Sonobe leg.; *Eleutherococcus spinosus* (leaf petiole and petiolule galls); HIC, NHC, dry, slide mounted and in ethanol. 29 immatures; same data but 10 Oct 2023; NHC, slide mounted and in ethanol. 18♂ 7♀; Honshu, Tochigi Pref., Utsunomiya City, Shimotokami-cho; 36.527 N, 139.846 E, 100 m; 16 Oct. 2015; Rikio Sonobe leg.; *Eleutherococcus spinosus* (leaf petiole and petiolule galls); HIC, dry mounted and in ethanol. 46 immatures, same data but 10 Oct. 2023; HIC, in ethanol. 1♂; Honshu, Tochigi Pref., Utsunomiya City, Nagaoka-cho; 36.593 N, 139.881 E, 150 m; 13 Oct. 2015; Rikio Sonobe leg.; *Eleutherococcus spinosus*; HIC, in ethanol.

Description. *Adult* (Figs 8A, 9, 10). Coloration. Body color yellowish. Antennae yellow with apices of segments 4 to 6 dark brown, and entire segments 7 to 10 black. Compound eyes dark brown. Ocelli orange. Legs brown. Forewing pale yellow, transparent, with pale brown patch around clavus. Hindwing transparent, except clavus brown.

Structure. Body medium-sized, length from anterior head margin to tip of folded forewing 4.8–5.1 mm, female generally larger (Fig. 8A); covered in short fine setae. Head (Fig. 9A) slightly narrower than thorax. Vertex width 1.7 x length, with short pubescence. Genal processes prominent, length along mid-line 0.8 x vertex length, divergent, conical, subacute at apex, medium-long pubescence. Antenna (Fig. 9A) length approximately 1.5 x head width, antennal segment 3 approximately double length of segment 4, relative length of flagellar segments as 1.0: 0.5: 0.3: 0.3: 0.3: 0.3: 0.2: 0.2; two unequal terminal setae: longer seta 1.1 x, and short truncate seta 0.2 x, segment 10 length. Thorax moderately arched dorsally, minutely pubescent. Hind leg (Fig. 9D) metatibia length 1.0–1.1 x head width. Forewing broad (Fig. 9B), length 5.7 x head width, and 2.5 x width, widest slightly distal to the middle; wing apex subacute; vein Rs very long, sinuous and curved to apical margin; vein M evenly curved with bifurcation anterior to line connecting apices of veins Rs and Cu_{1a}; cell m₁ slightly larger than cell cu₁; vein Cu_{1a} evenly curved, vein Cu_{1b} more or less straight; veins minutely pubescent. Hindwing (Fig. 9C) 0.7 x as long and 0.5 x as wide as forewing.

Male terminalia (Fig. 10A–C). Proctiger short, with slight posterior lobes reaching maximum expansion in the basal half, covered in long setae except for basal third laterally (Fig. 10A). Subgenital plate subglobular, with medium long setae laterally; posterior dorsal margin slightly convex. Paramere (Fig. 10B) longer than proctiger; in profile more or less parallel sided and straight, irregularly narrowing to apex which is acute and directed inward and rearward; inner face beset with long setae. Distal aedeagus segment (Fig. 10C) distinctly shorter than paramere (Fig. 16), markedly curved medially with broad semi-circle projections, apical portion inflated into a broadly curved hook with bluntly rounded apex; sclerotized end tube of ductus ejaculatorius short, slightly sinuous. Female terminalia (Fig. 10D) cuneate, slender; proctiger narrowing in apical fourth with acute apex, dorsal margin straight, only slightly longer than subgenital plate, with long setae in the apical half, anal ring length one fourth proctiger length, consisting of a single row of pores. Subgenital plate, in profile, triangular, apex acute, beset with long hairs laterally and ventrally. Ovipositor dorsal valvulae cuneate, ventral valvulae straight apparently without serrations apically.

Fifth instar immature (Fig. 11). Coloration. General color yellow. Forewing pad and thorax also yellow. Body (Fig. 11A) length 1.3 x width. Body surface, including margin of head, wing pads (Fig. 11C), caudal plate and legs

covered with sparsely distributed medium-short to long simple setae. Antenna (Fig. 11E) relative length of antennal segments 3 to 8 as 1.0: 0.7: 0.3: 0.6: 0.4: 1.8. Legs (Fig. 11A–B) as for generic description. Forewing pad length 2.7 x width, and 2.5–2.7 x antenna length. Caudal plate length 0.8 x width. Circumanal ring (Fig. 11D) peanut-shaped (medial constriction from anterior and posterior), width 0.3 x caudal plate width; outer ring composed of a single narrow row of elongate pores, inner ring composed of elongate pores.

Host plant. *Eleutherococcus spinosus* in Japan (Shinji, 1940); several other *Eleutherococcus* spp. (*E. divaricatus*, *E. sieboldianus*, *E. nodiflorus*) have been mentioned for South Korea (Kwon 1983; Kwon & Kwon 2020) but both hosts and distribution records remain doubtful (see Cho *et al.* 2017) or need to be confirmed.

Biology. Induces multi-chambered, spindle-shaped galls on the leaf petiole, petiolules and rarely on young twigs (Shinji 1940; Miyatake 1996).

Distribution. Japan (Shinji 1940; Miyatake 1996), South Korea (according to Kwon & Kwon 2020, but needs confirmation; see Cho *et al.* 2017).

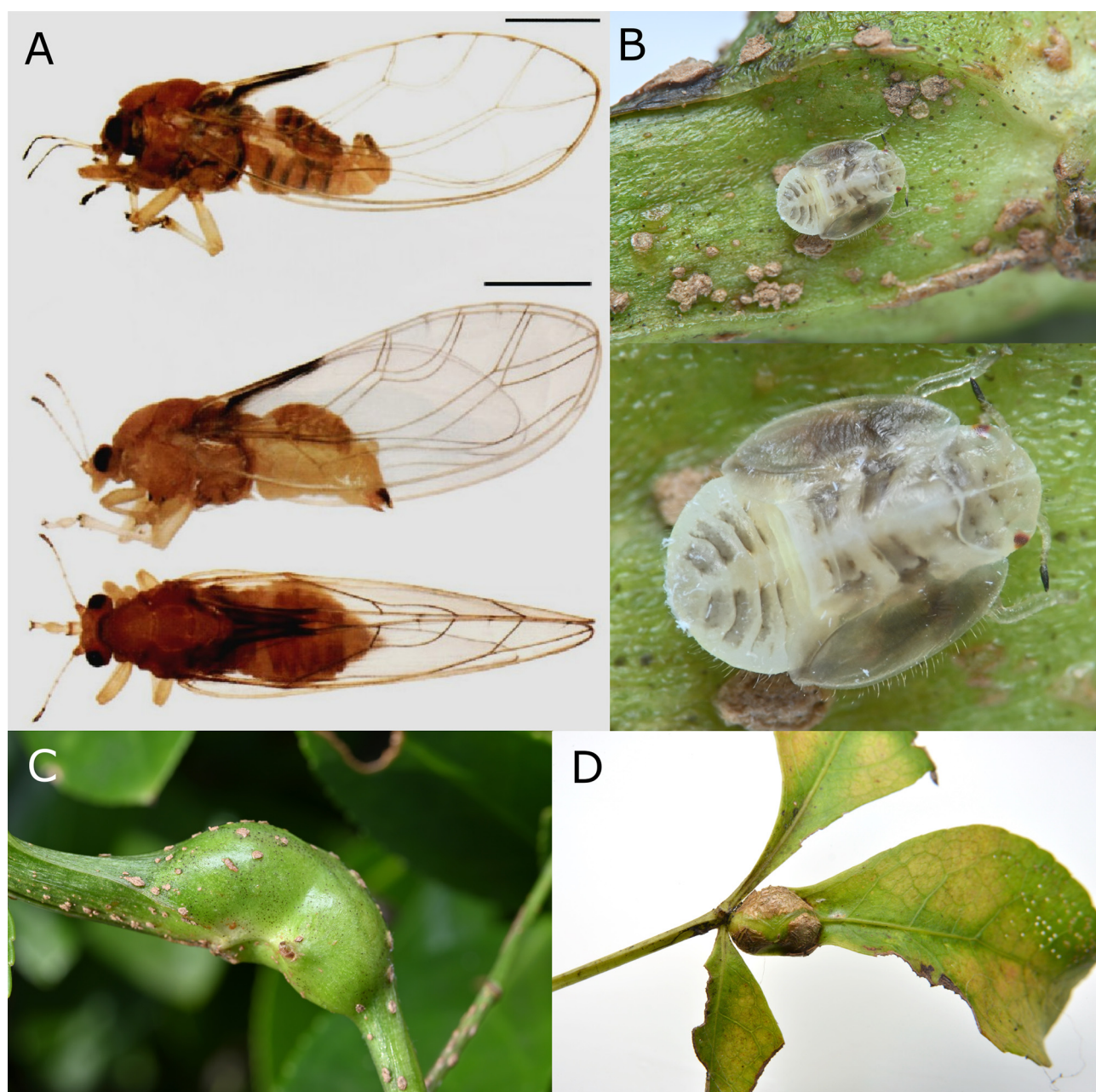


FIGURE 8. *Trioizidus ukogi* adults, immature and galls on *Eleutherococcus spinosus*. **A**, adults (male above), female (lateral and dorsal views, below) (images: Yorio Miyatake); **B**, immature within gall chamber (above) detail of immature (below); **C**, closed “spindle-shaped” gall on the petiole; **D**, petiolule gall. Scale bar in A 1 mm.

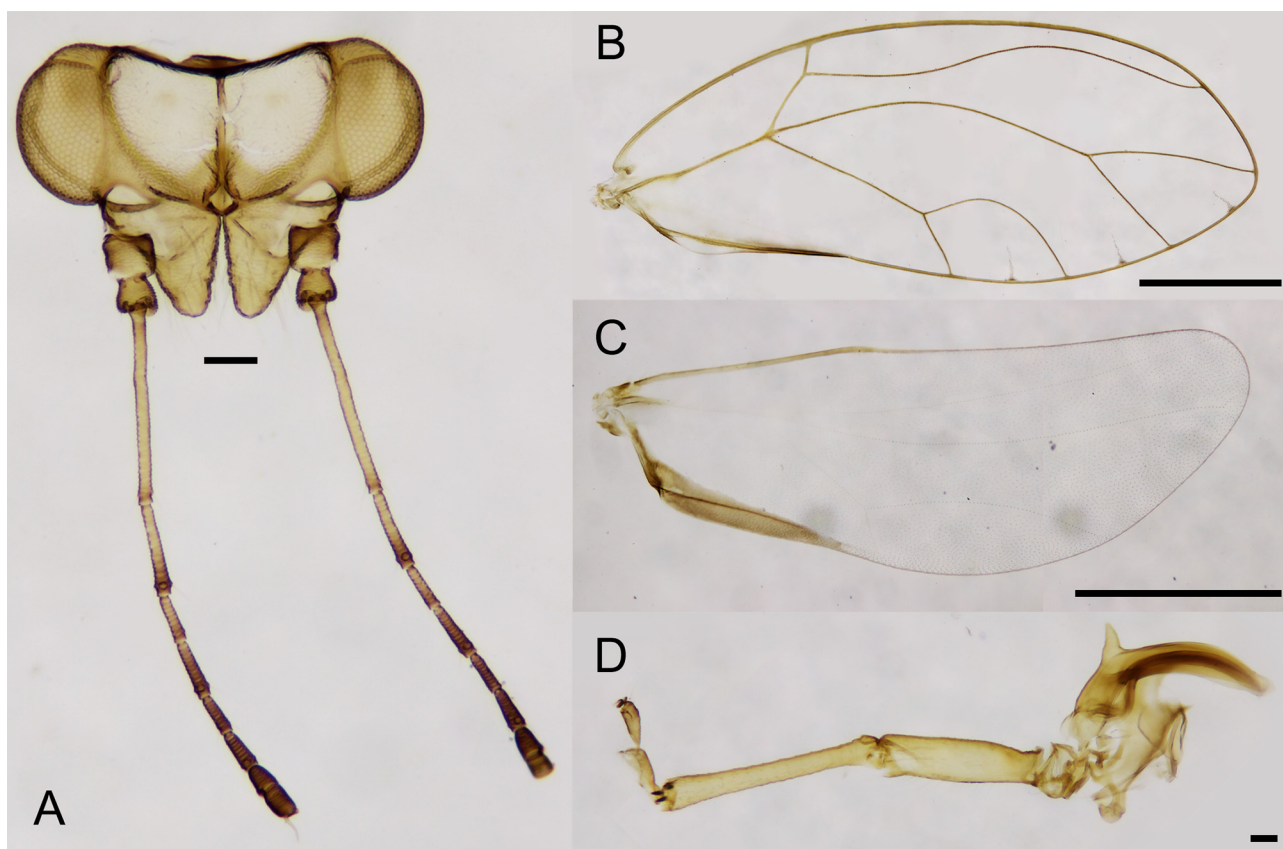


FIGURE 9. Adult *Triozidus ukogi* **comb. nov.** **A**, head and antennae; **B**, forewing; **C**, hindwing; **D**, hind leg. Scale bars: 0.1 mm (A, D); 1 mm (B, C).



FIGURE 10. Terminalia of *Triozidus ukogi* **comb. nov.** **A**, male terminalia (lateral view); **B**, paramere (inner surface); **C**, distal portion of aedeagus showing medial broadly semicircular projections (arrowed); **D**, female terminalia (lateral view). Scale bars: 0.1 mm.

Comment. We only examined material from Japan. Occurrences reported for South Korea were partly misidentification of *Triozidus stackelbergi* (see Cho *et al.* 2017; Kwon & Kwon 2020). Kwon & Kwon (2020) list this species as a pest on medicinal *Eleutherococcus* spp. in South Korea.

Genetic resources. Adult sequences of COI were all slightly divergent, three haplotypes: PQ817987–PQ817989.

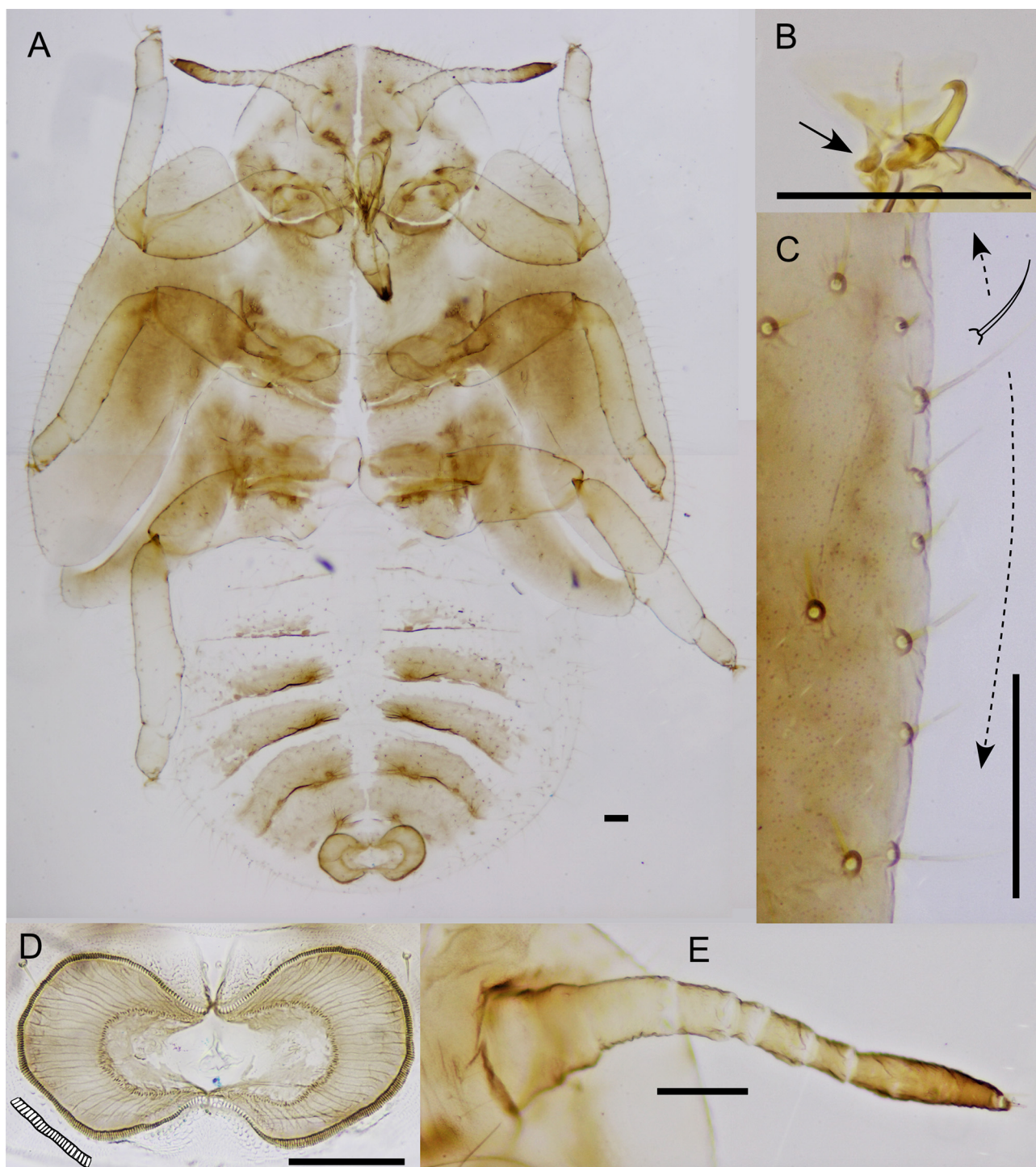


FIGURE 11. Fifth instar immature of *Triozidus ukogi* **comb. nov.** **A**, habitus; **B**, tarsal arolium showing asymmetric development of tarsal claws (vestigial claw arrowed); **C**, forewing pad marginal simple setae; **D** circumanal ring showing single narrow row of elongate pores (inset); **E** antenna. Scale bars: 0.1 mm.

***Triozidus yangorum* Liao & Percy sp. nov.**

(Figs 1C–F, 12–15)

Type material. **Holotype:** TAIWAN • ♂; Taipei City, Shilin, Guzhen; 25°08'06.4"N, 121°35'28.1"E; 17 Jan 2023; Y. C. Liao leg.; *Eleutherococcus trifoliatus*; NCHU, dry mounted. **Paratypes:** TAIWAN • 15♂, 19♀, 15 immatures; same data as for holotype. 2♂, 2♀; same data as for holotype, but NHMB. 7 immatures; Nantou Co., Meifeng;

24°05'21"N, 121°10'23"E; 23 Sep. 2008; M. M. Yang leg.; *Eleutherococcus trifolius*; NCHU, dry, slide mounted and in ethanol. **Other material examined:** TAIWAN • 1♂, 14 immatures; Nantou Co., Sitou Forest Recreation Area; 23.66513 N, 120.79718 E; 1295 m; 26 Jan. 2010; D. M. Percy leg.; *Eleutherococcus trifolius*; DMPC, slide mounted.

Description. *Adult* (Figs 1C, 12–14). Coloration. Body color yellowish brown (Figs 1C, 12). Newly emerged individuals light green. Entire head and abdominal tergites mid-brown. Antennae yellow with apices of segments 4, 6 and 8 dark brown, and entire segments 9 and 10 black. Compound eyes dark brown. Ocelli orange. Legs brown. Forewing pale yellow, transparent, with dark brown patch around clavus. Hindwing transparent, except clavus dark brown.

Structure. Body large-sized, length from anterior head margin to tip of folded forewing 5.3–6.1 mm, female generally larger (Fig. 12); covered in short fine setae. Head (Figs 12, 13A) slightly narrower than thorax. Vertex width 1.8–2.0 x length, minutely pubescent. Genal processes prominent, length along mid-line 0.7–0.8 x vertex length, divergent, conical, blunt at apex, medium-long pubescence. Antenna (Figs 13B–C) length 1.8–1.9 x head width, antennal segment 3 approximately double length of segment 4, relative length of flagellar segments as 1.0: 0.5: 0.3: 0.3: 0.3: 0.3: 0.2: 0.2; two unequal terminal setae: longer seta 1.1 x, and shorter, truncate seta 0.2 x segment 10 length. Thorax moderately arched dorsally, minutely pubescent. Hind leg (Fig. 13F) metatibia length 1.0–1.1 x head width. Forewing broad (Fig. 13D), length 6.1–6.8 x head width, and 2.4–2.6 x width, widest slightly distal to the middle; wing apex acute; vein Rs moderately long, gradually curved to fore margin; vein M evenly curved with bifurcation at or slightly anterior to line connecting apices of veins Rs and Cu_{1a}; cell m₁ larger than cell cu₁; vein Cu_{1a} evenly curved, vein Cu_{1b} more or less straight; veins minutely pubescent. Hindwing (Fig. 13E) 0.6 x as long and 0.5 x as wide as forewing.

Male terminalia (Figs 14A–C). Proctiger short, with moderate posterior lobes reaching maximum extension in the apical half, covered in long setae except for basal third laterally (Fig. 14A). Subgenital plate subglobular, with medium long setae laterally and ventrally; posterior dorsal margin slightly convex. Paramere (Figs 14A–B) about as long as proctiger; in profile broader at base, sinuous, before narrowing to apex which is acute and directed inward and rearward; inner face beset with long setae, outer surface with shorter setae. Distal aedeagus segment (Fig. 14C) about as long as paramere (Figs 14A, 16), angled medially with thumb-shaped projections, apical portion inflated into a shallow hook with blunt apex; sclerotized end tube of ductus ejaculatorius short, slightly sinuous. Female terminalia (Fig. 14D) cuneate, short; proctiger dorsal margin slightly sinuate with medial depression and acute apex, only slightly longer than subgenital plate, with long setae in the apical half, anal ring length approximately one third proctiger length, consisting of a single row of pores. Subgenital plate, in profile, triangular, apex acute, beset with long hairs laterally and ventrally. Ovipositor dorsal valvulae cuneate, ventral valvulae straight with several shallow serrations apically.

Measurements (range, mean±SD) in mm (5 males, 5 females). Body length (including forewing) ♂ 5.38–5.81, 5.63±0.17; ♀ 5.25–6.06, 5.81±0.32. Head width ♂ 0.74–0.78, 0.76±0.02; ♀ 0.76–0.80, 0.77±0.02. Vertex width ♂ 0.41–0.43, 0.42±0.01; ♀ 0.38–0.43, 0.41±0.02. Vertex length ♂ 0.23–0.30, 0.26±0.03; ♀ 0.28–0.29, 0.28±0.01. Genal cone length ♂ 0.19–0.22, 0.20±0.01; ♀ 0.20–0.23, 0.21±0.01. Antenna length ♂ 1.40–1.50, 1.44±0.04; ♀ 1.33–1.35, 1.34±0.01. Metatibia length ♂ 0.80–0.85, 0.82±0.03; ♀ 0.73–0.88, 0.81±0.06. Forewing length ♂ 4.58–4.93, 4.76±0.20; ♀ 4.85–5.56, 5.18±0.38. Forewing width ♂ 1.89–1.98, 1.93±0.04; ♀ 1.96–2.19, 2.06±0.11. Aedeagus length 0.30 (n=1). Paramere length 0.30 (n=2). Proctiger length ♀ 0.45–0.50 (n=2). Subgenital plate length ♀ 0.46–0.50 (n=2).

Fifth instar immature (Figs 1D, 15). Coloration. General color yellow. Forewing pad and thorax pale brown. Body (Fig. 15A) length 1.3–1.4 x width. Body surface, including margin of head, wing pads (Fig. 15C), caudal plate and legs covered with medium dense, long simple setae. Antenna (Fig. 15E) relative length of antennal segments 3 to 8 as 1.0: 0.85: 0.3: 0.4: 0.3: 1.8. Legs (Figs 15A–B) as for generic description. Forewing pad length 2.8–3.2 x width, and 2.4–2.8 x antenna length. Caudal plate length 0.8–1.0 x width. Circumanal ring (Fig. 15D) heart-shaped (medial constriction mainly from anterior); width 0.3 x caudal plate width; outer ring mostly composed of a single row of elongate pores, with occasional convolutions and intermittent multi-pore sections; inner ring composed of a mixture of small and irregular pores.

Measurements (range, mean±SD) in mm (5 immatures). Body length 2.53–2.88, 2.70±0.15. Head width 0.80–0.85, 0.81±0.02. Antenna length 0.53–0.61, 0.57±0.03. Metatibiotarsus length 0.71–0.80, 0.76±0.04. Forewing pad length 1.36–1.60, 1.48±0.11. Caudal plate length 0.90–1.25, 1.01±0.14. Caudal plate width 1.08–1.18, 1.16±0.06. Circumanal ring width 0.30–0.35, 0.32±0.02.

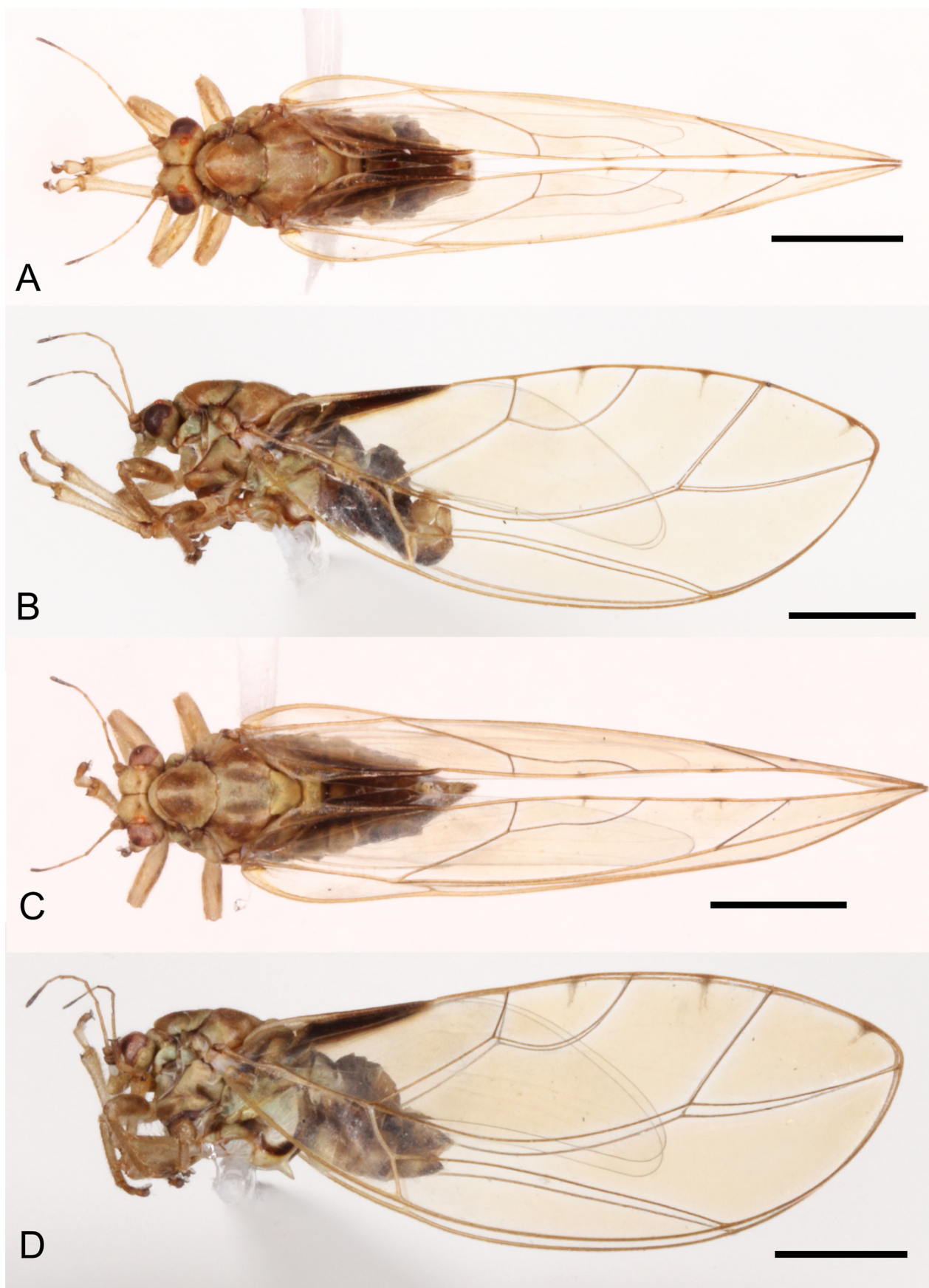


FIGURE 12. Adults of *Triozidus yangorum* **sp. nov.** **A**, Holotype, male, dorsal view; **B**, Holotype, male, lateral view; **C**, female, dorsal view; **D**, female, lateral view. Scale bars: 1 mm.

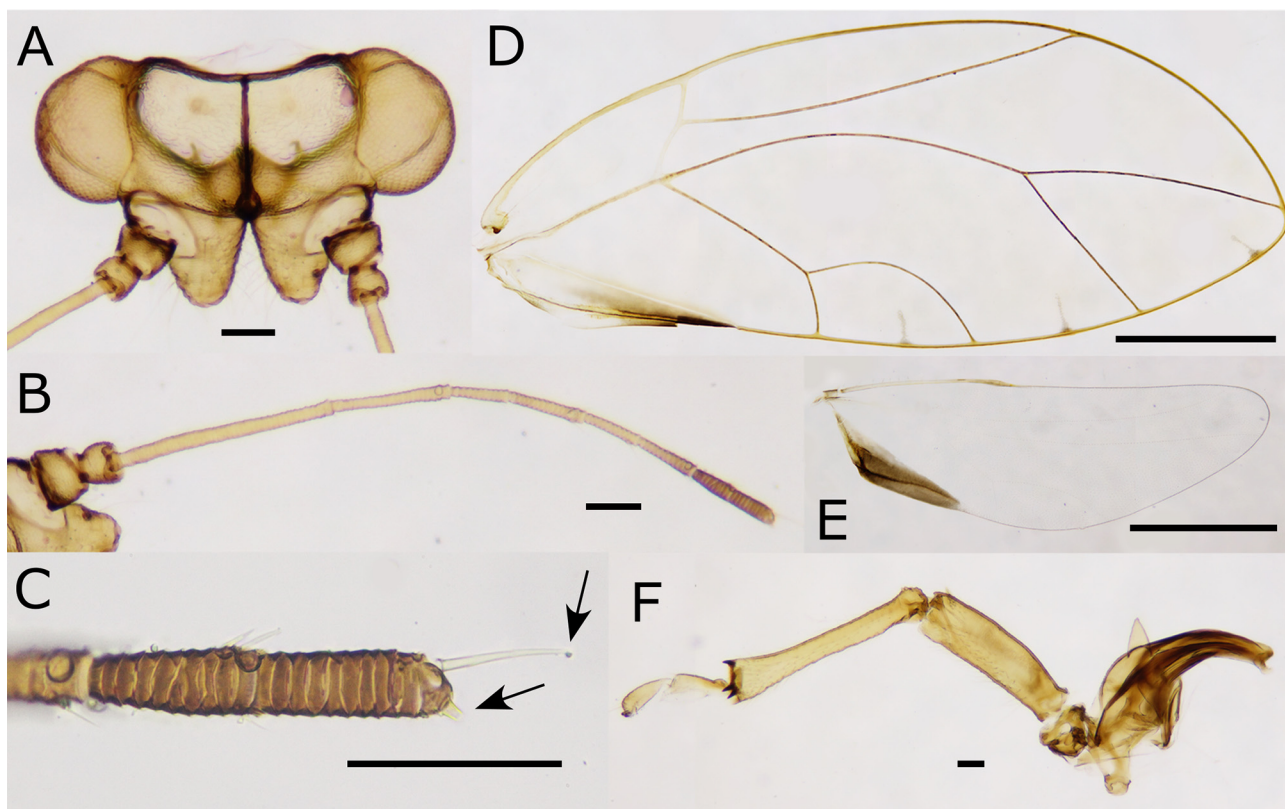


FIGURE 13. Adult *Triozidus yangorum* sp. nov. **A**, head; **B**, antenna; **C**, terminal antennal segments showing uneven length terminal setae (arrowed); **D**, forewing; **E**, hindwing; **F**, hind leg. Scale bars: 0.1 mm (A, B, C, F); 1 mm (D, E).

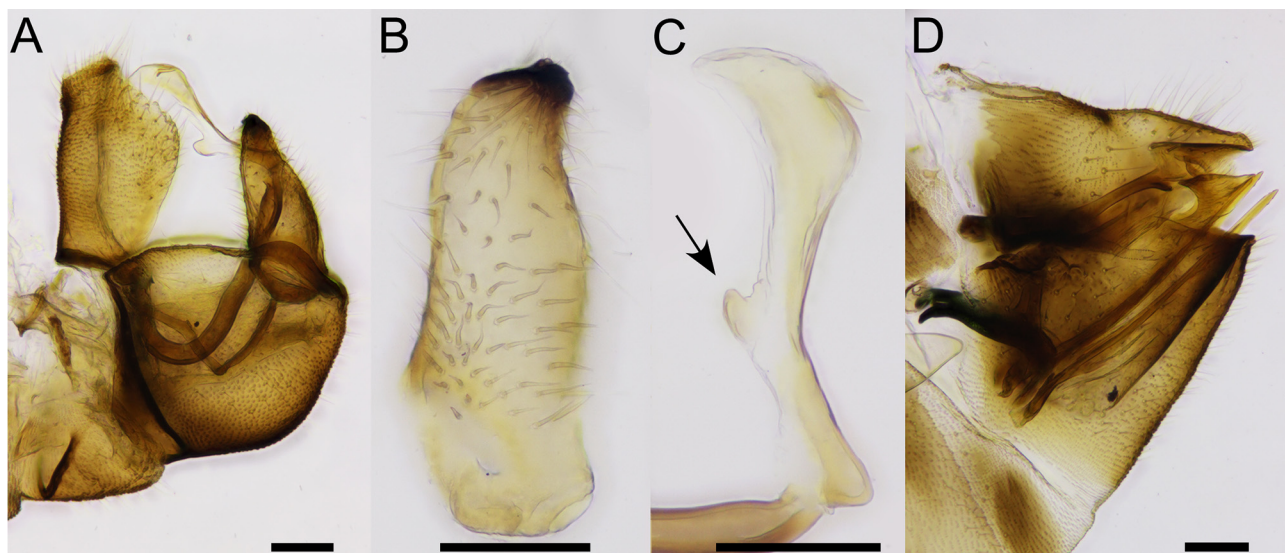


FIGURE 14. Terminalia of *Triozidus yangorum* sp. nov. **A**, male terminalia (lateral view); **B**, paramere (inner surface); **C**, distal portion of aedeagus, showing medial narrow thumb-like projections (arrowed); **D**, female terminalia (lateral view). Scale bars: 0.1 mm.

Etymology. The specific name honours both Prof. Chung-Tu Yang and Dr. Man-Miao Yang for their enormous contribution to the systematics of Psylloidea.

Distribution. Taiwan; only found in the central and northern part.

Host plant. *Eleutherococcus trifoliatus* (Araliaceae).

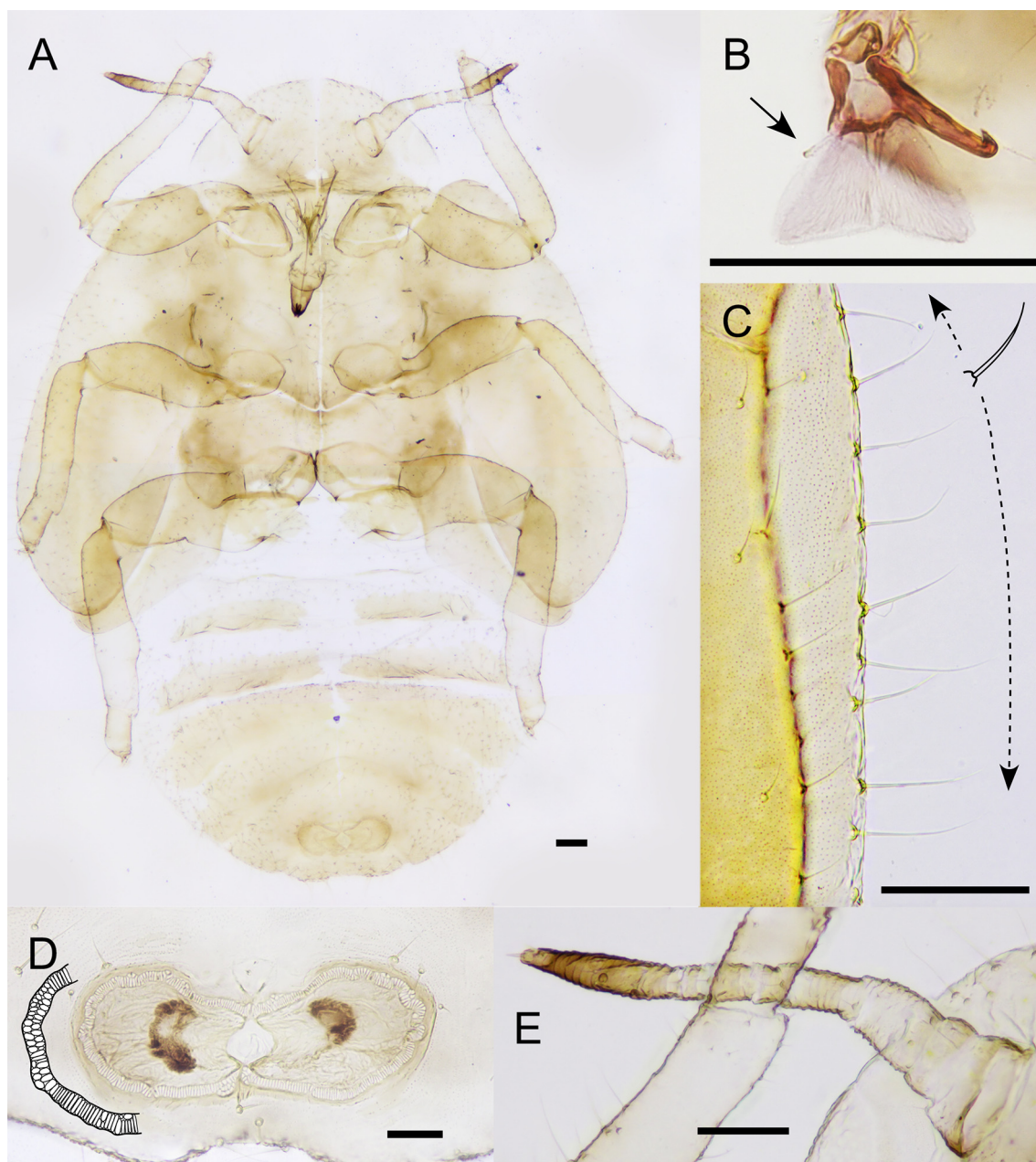


FIGURE 15. Fifth instar immature of *Triozidus yangorum* sp. nov. **A**, habitus; **B**, tarsal arolium showing asymmetric development of tarsal claws (vestigial claw arrowed); **C**, forewing pad marginal simple setae; **D**, circumanal ring showing intermittent irregular pore shape (inset); **E**, antenna. Scale bars: 0.1 mm.

Biology. Univoltine with adults emerging December to January. Immatures develop within large, fully enclosed round galls that are positioned just below the base of leaflets on the petiolules. Occasionally galls are seen on the leaflet base, but this seems to be a secondary oviposition preference. Each gall consists of a single gall chamber with usually a single immature (Fig. 1D). Galls are found individually or in aggregates of two to four galls per leaf, often with a gall on each of the three petiolules (Figs 1E–F). The host plant, *E. trifoliatum*, is found in montane zones (500 to 1,500 m elevation) as an understory forest plant with prickly stems and a sprawling or scandent habit.

Genetic resources. Adult and immature sequences were identical: annotated mitochondrial genome: Genbank PQ826428.

Nomenclatural acts

The following new nomenclatorial acts are proposed in this work:

New taxa

Triozidus burckhardti Liao & Percy **sp. nov.**

Triozidus yangorum Liao & Percy **sp. nov.**

New combinations

Triozidus Li, 1994 **stat. rev.**

Triozidus ceratophorus (Li, 2005) **comb. nov.** from *Heterotrioza*

Triozidus eleutherococci (Konovalova, 1980) **comb. nov.** from *Trioza*

Triozidus stackelbergi (Loginova, 1967) **comb. nov.** from *Heterotrioza*

Triozidus ukogi (Shinji, 1940) **comb. nov.** from *Heterotrioza*

Results of molecular analyses

Support for the monophyly of *Triozidus sensu novo* as redefined here is strong (> 90 %) in both the ML backbone constraint analysis and the COI fragment analysis. The four *Triozidus* species for which we obtained molecular data were recovered in the ML backbone constraint analysis in the configuration (*T. yangorum* (*T. stackelbergi* (*T. burckhardti*, *T. ukogi*))). However, the infrageneric bootstrap support for grouping *T. burckhardti* and *T. ukogi* as sister taxa is only moderate (75 %) and this analysis is likely affected by the use of the two non-overlapping COI fragments. The NJ analysis of the COI data (714 bp fragment) recovers a different configuration (*T. stackelbergi* (*T. yangorum*, *T. ukogi*)), but also with weak support for *T. yangorum* and *T. ukogi* as sister taxa (< 60 %) (Fig. 16) (as the 850 bp COI fragment sequenced for *T. burckhardti* is nonoverlapping, it was excluded from this analysis). In both analyses, the internal branch lengths between species within *Triozidus* were short, possibly reflecting rapid early divergence in the evolutionary history of the genus. Interspecific genetic distances between *Triozidus* species based on COI were relatively high: 10.6–12.5% divergence. Three of the *Triozidus* species for which multiple individuals were sampled, *T. burckhardti*, *T. yangorum* and *T. stackelbergi*, recovered a single haplotype for each species. The three individuals of *T. ukogi* each had a different haplotype but with minimal genetic variation (< 0.5% COI divergence) (Fig. 16). The lack of, or minimal, haplotype diversity is expected as all four taxa were sampled from a single population.

Triozidus stackelbergi and *T. ukogi* were originally placed in the catch-all, polyphyletic genus *Trioza* and subsequently transferred to *Heterotrioza* (Klimaszewski 1973; Li 2011; Kwon & Kwon 2020; Cho *et al.* 2022); moreover Klimaszewski (1973) had included both species in *Dyspersa* Klimaszewski as a subgenus of *Heterotrioza*. The mitogenome analyses of Percy *et al.* (2018) placed *Triozidus* (as “MERGE016-Genus sp”) within Triozidae Group B, whereas the type species of *Trioza*, *T. urticae* (Linnaeus, 1758), representing genus *Trioza sensu stricto*, is placed in Group M, *Heterotrioza sensu stricto* in Group D, and *Dyspersa sensu stricto* (as in Cho *et al.* 2022) in Group A (see Fig. 16). The genera found to be most closely related to *Triozidus* within Group B (in both Percy *et al.* 2018 and this study) are *Lauritrioza* and two generic groups not yet formerly named. One of these is a primarily Lauraceae-feeding group (including *Trioza anceps* Tuthill, 1944, *T. magnoliae* (Ashmead, 1881), *T. ulei* (Rübsaamen, 1908)) labelled “Aconoza” in Fig. 16 which refers to *Bactericera* (*Aconoza*) *sensu* Rübsaamen (1908) (see Burckhardt & Queiroz 2012). Bootstrap support for the placement and monophyly of *Triozidus* within this subgroup in Triozidae Group B is strong (> 90 %) in both the ML and NJ analyses (Fig. 16).

Sequences have been deposited in Genbank with accession numbers PQ817986–PQ817989 (for the unique COI haplotypes recovered for *T. stackelbergi* and *T. ukogi*), and PQ817990/PQ817253 (for COI and cytB respectively for *T. burckhardti*), and the annotated mitochondrial genome of *Triozidus yangorum* is deposited in Genbank with accession number PQ826428.

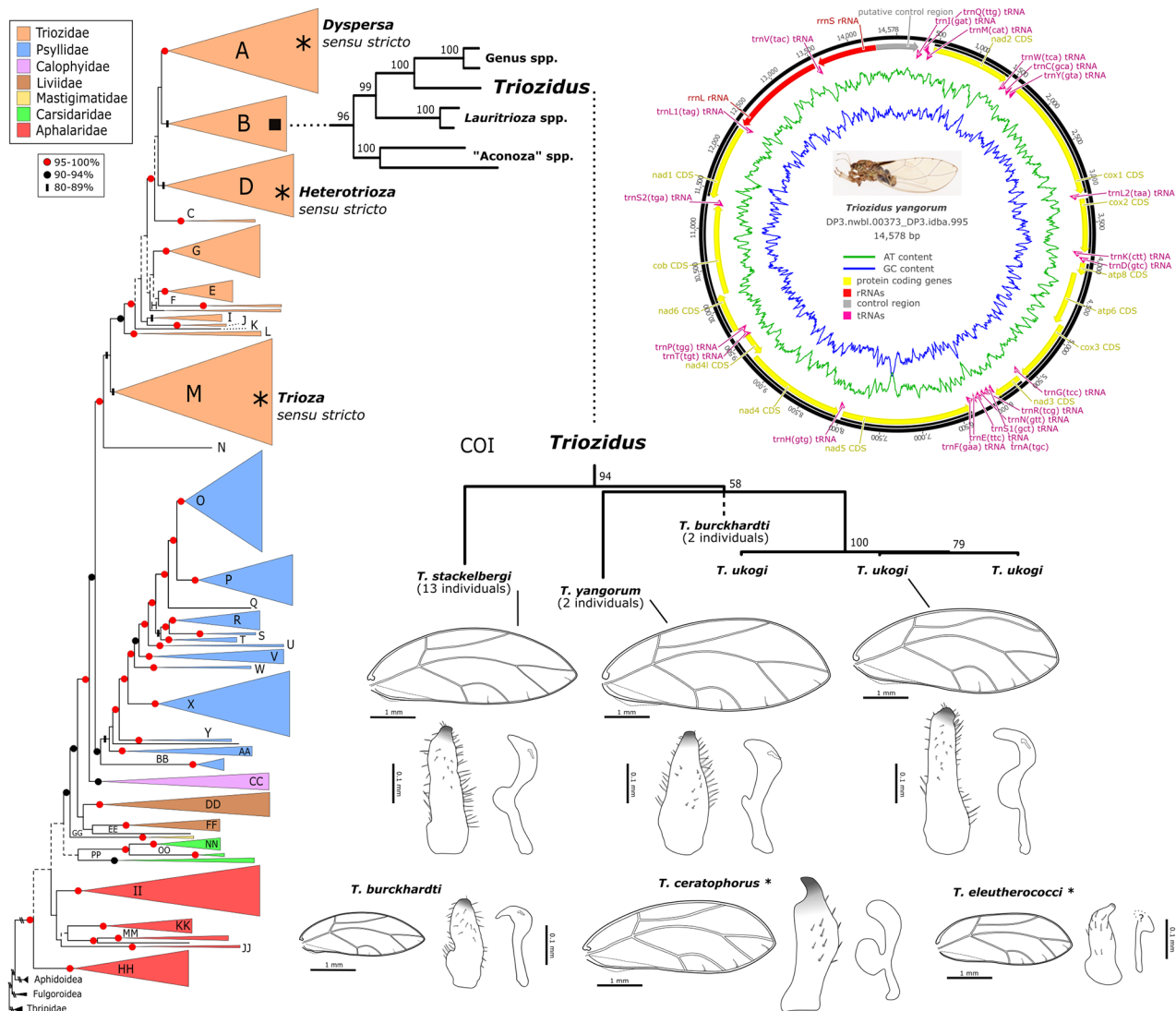


FIGURE 16. Phylogenetic placement of *Trioizidus* in family Triozidae is indicated by a black square representing a subgroup within Group B (see Percy *et al.* 2018), the related genera are expanded on in the text. An asterisk indicates the placement of the type species of *Heterotrioza*, *H. chenopodii* in Group D, and *Trioza*, *T. urticae* in Group M, and *Dyspersa sensu* Cho *et al.* (2022) in Group A. Configuration of the three *Trioizidus* taxa to one another based on the 714 bp COI fragment data (unique haplotypes only) is shown, with *T. burckhardti* placement indicated based on the backbone analysis (see text); taxon placements within *Trioizidus* are uncertain in both analyses due to short internal branches and low to moderate bootstrap support, with a slightly different taxon configuration recovered in the ML backbone constraint analysis (see text). Illustrations of forewing, paramere and aedeagus are shown for all six *Trioizidus* species to indicate comparative sizes; an asterisk by *T. ceratophorus* and *T. eleutherococci* indicates the illustrations are redrawn with reference to Li (2011) and Konovalova (1980, 1988) respectively, and in these cases paramere and aedeagus may not be to scale, plus the apex of the aedeagus is partly obscured in the illustration for *T. eleutherococci*. The annotation of the mitogenome of *T. yangorum* is graphically represented at top right.

Discussion

Trioizidus, as redefined here, is a small genus whose placement within the phylogenetic structure of the family Triozidae and monophyly is well supported by molecular data in Percy *et al.* (2018) and the current study. The five genera, *Dyspersa*, *Heterotrioza*, *Lauritrioza*, *Trioza* and *Trioizidus*, were included in the mitogenome analysis of Percy *et al.* (2018), and the genera in which *Trioizidus* species were previously placed (namely *Dyspersa*, *Heterotrioza*, *Trioza*) are not close in the Triozidae phylogeny, with each genus being found in a different major group within the family

(see Fig. 16). A number of distinguishing characters in *Triozidus* are typical but not universal, and the paucity of macromorphological synapomorphies for the genus makes reliance on the molecular data more critical. Fortunately, the mitogenome phylogenetic resolution is unambiguous. The molecular COI data is not particularly helpful for determining relationships within the genus, possibly due to a rapid early diversification resulting in short internal branch lengths coupled with considerable divergences between species; but based on morphology, we consider there to be two subgroups characterized by presence/absence of the bipartite projection on the distal aedeagus segment. The group without this character currently includes *T. buckhardti* and *T. eleutherococci*, but another taxon originally described by Li (1994) in *Triozidus*, *Heterotrioza flaviscutatus* (Li, 1994), may also belong in *Triozidus sensu novo*, however, insufficient information is available at this time, and we flag this for future research.

Each of the *Triozidus* species are readily distinguished from one another by adult characters and DNA barcode data. The immatures are similar, as is often the case in congeneric closed gall taxa (Percy 2017) and are most easily distinguished by chaetotaxy and the shape of the circumanal ring. Immatures of closed gall taxa often have reduced sclerites, but this is only moderately the case in *Triozidus* immatures. The unusual morphology of the distal aedeagus segment with the bipartite medial projection (found in all taxa except *T. burckhardti* and *T. eleutherococci*) is not found elsewhere in Triozidae, and together with the asymmetric development of the immature tarsal claws, provide two distinct morphological characteristics considered typical for the genus. Neither the aedeagus projections nor the tarsal claw character have obvious functional explanations, but variation in overall tarsal claw size is often associated with gall biology shifts (e.g., Percy 2017), so it is likely that a vestigial tarsal claw arose in conjunction with the evolution of the galling habit in *Triozidus*.

All *Triozidus* (where host plant is known) are found on the same host plant genus, *Eleutherococcus*, which is widespread in eastern Asia in mostly temperate to subtropical zones (POWO 2024). With 29 species of *Eleutherococcus* in this region (POWO 2024), further surveys may reveal additional species of *Triozidus*. Interestingly, three of the *Eleutherococcus* species used as hosts by *Triozidus* (*E. divaricatus*, *E. sessiliflorus*, and *E. trifoliatum*) were shown to have low molecular variation among taxa based on nuclear ITS data (Kim *et al.* 2014), although the picture of variation is complicated by multiple gene copies and a possible history of hybridization and horizontal gene transfer (Song *et al.* 2012). The genus *Eleutherococcus* is considered relatively young, less than six million years old, with early divergence within *Eleutherococcus* occurring less than four million years ago (Kim *et al.* 2017), although an older time frame has also been proposed (see Li & Wen 2016). A recent evolutionary timescale for the divergence of *Eleutherococcus* coupled with the mitochondrial divergence within *Triozidus* found in this study (10.6–12.5% based on COI data) would suggest that *Triozidus* was co-diversifying over a similar time period as the host genus. However, given how closely related some of the *Eleutherococcus* species are, and the occurrence of some *Triozidus* on multiple different *Eleutherococcus* species, any apparent host specificity within the host genus may be more a product of opportunism and geographical isolation. This would also partly explain why *T. stackelbergi* occurs on different *Eleutherococcus* host species in different regions, and may also explain the expanded host ranges that have been reported where the species are introduced (Kwon & Kwon 2020). Similarly, the gall position, although seemingly fixed in some *Triozidus*, is highly variable in others (e.g., *T. stackelbergi*). In other words, closely related *Eleutherococcus* species may all be suitable hosts for *Triozidus* taxa, and if this is the case, host selection is more likely determined by opportunity and/or lack of choice than by canalized specificity.

Acknowledgements

We are grateful to Yueh-Yun Tang for her help in the field and Bao-Cheng Lai for his assistance in the slide mounting. We thank Geonho Cho for providing specimens of *T. stackelbergi* from South Korea, Akihide Koguchi and Rikio Sonobe for providing the Japanese material of *T. stackelbergi* and *T. ukogi*, respectively, and Yorio Miyatake for providing images of *T. ukogi* habitus and gall. We thank Maria Kuzmina for providing a translation of Loginova's Russian description of *Trioza stackelbergi*. DP is grateful to Quentin Cronk for providing laboratory facilities at the University of British Columbia. We gratefully acknowledge reviews from Daniel Burckhardt and an anonymous reviewer which greatly improved this manuscript, and we thank David Ouvrard for editorial guidance.

References

- Ashmead, W.H. (1881) On the Aphididae of Florida, with descriptions of new species. *Canadian Entomologist*, 13, 220–225.
<https://doi.org/10.4039/Ent13220-11>
- Bastin, S., Burckhardt, D., Reyes-Betancort, J.A., Hernández-Suárez, E. & Ouvrard, D. (2023) A review of the jumping plant-lice (Hemiptera: Psylloidea) of the Canary Islands, with descriptions of two new genera and sixteen new species. *Zootaxa*, 5313 (1), 1–98.
<https://doi.org/10.11646/zootaxa.5313.1.1>
- Burckhardt, D. (2005) Biology, ecology, and evolution of gall-inducing psyllids (Hemiptera: Psylloidea). In: Raman, A., Schaefer, C. & Withers, T. (Eds.), *Biology, Ecology and Evolution of Gall-inducing Arthropods*. Science Publishers, Enfield, pp. 143–157.
- Burckhardt, D. & Basset, Y. (2000) The jumping plant-lice (Hemiptera, Psylloidea) associated with *Schinus* (Anacardiaceae): systematics, biogeography and host plant relationships. *Journal of Natural History*, 34, 57–155.
<https://doi.org/10.1080/002229300299688>
- Burckhardt, D. & Ouvrard, D. (2012) A revised classification of the jumping plant-lice (Hemiptera: Psylloidea). *Zootaxa*, 3509 (1), 1–34.
<https://doi.org/10.11646/zootaxa.3509.1.1>
- Burckhardt, D., Ouvrard, D. & Percy, D.M. (2021) An updated classification of the jumping plant-lice (Hemiptera: Psylloidea) integrating molecular and morphological evidence. *European Journal of Taxonomy*, 736, 137–182.
<https://doi.org/10.5852/ejt.2021.736.1257>
- Burckhardt, D. & Queiroz, D.L. (2012) Checklist and comments on the jumping plant-lice (Hemiptera: Psylloidea) from Brazil. *Zootaxa*, 3571 (1), 26–48.
<https://doi.org/10.11646/zootaxa.3571.1.2>
- Cho, G., Burckhardt, D. & Lee, S. (2017) On the taxonomy of Korean jumping plant-lice (Hemiptera: Psylloidea). *Zootaxa*, 4238, 531–561.
<https://doi.org/10.11646/zootaxa.4238.4.3>
- Cho, G., Burckhardt, D. & Lee, S. (2022) Check list of jumping plant-lice (Hemiptera: Psylloidea) of the Korean Peninsula. *Zootaxa*, 5177 (1), 001–091.
<https://doi.org/10.11646/zootaxa.5177.1.1>
- Hodkinson, I.D. (1974) The biology of the Psylloidea (Homoptera): a review. *Bulletin of Entomological Research*, 64, 325–338.
<https://doi.org/10.1017/S0007485300031217>
- Hodkinson, I.D. (1984) The biology and ecology of the gall-forming Psylloidea (Homoptera). In: Ananthakrishnan, T.N. (Ed.), *Biology of Gall Insects*. Arnold, London, pp. 59–77.
- Hodkinson, I.D. (2009) Life cycle variation and adaptation in jumping plant lice (Insecta: Hemiptera: Psylloidea): a global synthesis. *Journal of Natural History*, 43, 65–179.
<https://doi.org/10.1080/00222930802354167>
- Hollis, D. (1987) A review of the Malvales-feeding psyllid family Carsidaridae (Homoptera). *Bulletin of the British Museum (Natural History) Entomology Series*, 56, 87–127.
- Hollis, D. & Broomfield, P.S. (1989) *Ficus*-feeding psyllids (Homoptera), with special reference to the Homotomidae. *Bulletin of the British Museum (Natural History) Entomology Series*, 58, 131–183.
- Huang, Y.H., Li, J.T., Zan, K., Wang, J. & Fu, Q. (2022) The traditional uses, secondary metabolites, and pharmacology of *Eleutherococcus* species. *Phytochemistry Reviews*, 21, 1081–1184.
<https://doi.org/10.1007/s11101-021-09775-z>
- Kearse, M., Moir, R., Wilson, A., Stones-Havas, S., Cheung, M., Sturrock, S., Buxton, S., Cooper, A., Markowitz, S., Duran, C., Thierer, T., Ashton, B., Meintjes, P. & Drummond, A. (2012) Geneious Basic: an integrated and extendable desktop software platform for the organization and analysis of sequence data. *Bioinformatics*, 28, 1647–1649.
<https://doi.org/10.1093/bioinformatics/bts199>
- Kim, K., Nguyen, V.B., Dong, J., Wang, Y., Park, J.Y., Lee, S.C. & Yang, T.J. (2017) Evolution of the Araliaceae family inferred from complete chloroplast genomes and 45S nrDNAs of 10 *Panax*-related species. *Scientific Reports*, 7, 4917.
<https://doi.org/10.1038/s41598-017-05218-y>
- Kim, M-K., Jang, G-H., Yang, D-C., Lee, S., Lee, H-N. & Jin, C-G. (2014) Molecular authentication of *Acanthopanax* Cortex by multiplex-PCR analysis tools. *Korean Journal of Plant Resources*, 27, 680–686.
<https://doi.org/10.7732/kjpr.2014.27.6.680>
- Klimaszewski, S.M. (1973) The jumping plant lice or psyllids (Homoptera, Psylloidea) of the Palaearctic: an annotated checklist. *Annales Zoologici*, 30, 155–286.
- Konovalova, Z.A. (1980) New species of Psylloidea (Homoptera) from Primorye region. In: Ler, P.A. (Ed.), *Taksonomiya nasekomykh Dal'nego Vostoka [Taxonomy of insects of the Far East]*. Biologo-pochvennyi institut (Akademii nauk SSSR), Vladivostok, pp. 20–24. [in Russian]
- Konovalova, Z.A. (1988) Suborder Psyllinea – jumping plant lice. In: Ler, P.A. (Ed.), *Opredelitel' nasekomykh Dal'nego Vostoka SSSR v shesti tomakh. Vol. 2. Ravnokrylye i poluzhestkokrylye [Keys to the insects of the Far East]*. Biologo-pochvennyi

- institut (Akademii nauk SSSR), Nauka Publishing House, Leninigrad, pp. 1–46. [U.S. Department of Agriculture, 2001, English translation]
- Kuznetsova, V.G., Labina, E.S., Shapoval, N.A., Maryańska-Nadachowska, A. & Lukhtanov, V.A. (2012) *Cacopsylla fraudatrix* sp.n. (Hemiptera: Psylloidea) recognised from testis structure and mitochondrial gene COI. *Zootaxa*, 3547 (1), 55–63. <https://doi.org/10.11646/zootaxa.3547.1.5>
- Kwon, Y.J. (1983) Psylloidea of Korea (Homoptera: Sternorrhyncha). *Insecta Koreana*, Series 2, 1–181.
- Kwon, J.H. & Kwon, Y.J. (2020) Psylloidea. *Insect Fauna of Korea*, 9 (9), 1–403.
- Kwon, J.H., Suh, S.J. & Kwon, Y.J. (2022a) Notes on the trioqid jumping plant-louse, *Bactericera sarahae* Kwon et Kwon, associated with Oriental medicinal plant of *Acanthopanax* from Korea (Hemiptera: Psylloidea: Triozidae). *2022 Spring Meeting of The Entomological Society of Korea*, Conference Poster. Available from: <https://www.researchgate.net/publication/372768814> (accessed 12 March 2025)
- Kwon, J.H., Suh, S.J. & Kwon, Y.J. (2022b) A new jumping plant-louse genus, *Lunatrioza* gen. nov., split from *Heterotrioza* Dobreanu et Manolache belonging to the family Triozidae from Korea (Hemiptera: Psylloidea). *2022 Spring Meeting of The Entomological Society of Korea*, 2022, Conference Poster: Available from: <https://www.researchgate.net/publication/372768769> (accessed 21 November 2024)
- Li, F. (1994) New genus *Triozidus* and five new species from China (Homoptera: Psylloidea: Triozidae). *Wuyi Science Journal*, 11, 84–92. [in Chinese]
- Li, F. (2005) Homoptera: Psylloidea. In: Yang, X. (Ed.), *Insect Fauna of Middle-West Qinling Range and South Mountains of Gansu Province*. Science Press, Beijing, pp. 142–213. [in Chinese]
- Li, F. (2011) Psyllidomorpha of China (Insecta: Hemiptera). Science Press, Beijing, 1976 pp. [in Chinese]
- Li, R. & Wen, J. (2016) Phylogeny and diversification of Chinese Araliaceae based on nuclear and plastid DNA sequence data. *Journal of Systematics and Evolution*, 54, 453–467. <https://doi.org/10.1111/jse.12196>
- Linnaeus, C. (1758) *Systema naturae per regna tri naturae, secundum classes, ordines, genera, species, cum characteribus, differentiis, synonymis, locis. Tomus I. Editio decima, reformata*. Impensis Direct. Laurentii Salvii, Holmiae, Stockholm, 824 pp. <https://doi.org/10.5962/bhl.title.542>
- Loginova, M.M. (1967) New psyllids (Homoptera, Psylloidea) from the Far East of the USSR. *Entomologicheskoe Obozrenie*, 46, 336–347. [in Russian]
- Malenovsky, I., Burckhardt, D. & Tamesse, J.L. (2007) Jumping plant-lice of the family Phacopteronidae (Hemiptera: Psylloidea) from Cameroon. *Journal of Natural History*, 41, 1875–1927. <https://doi.org/10.1080/00222930701515488>
- Miller, M.A., Pfeiffer, W. & Schwartz, T. (2010) Creating the CIPRES Science Gateway for inference of large phylogenetic trees. *Proceedings of the Gateway Computing Environments Workshop (GCE)*, New Orleans, 2010, 1–8.
- Miyatake, Y. (1996) Psylloidea. In: Yukawa, J. & Masuda, H. (Eds.), *Insect and mite galls of Japan*. Zenkoku Nôson Kyôiku Kyôkai, Tokyo, pp. 352–358. [in Japanese]
- Ouvrard, D., Chalise, P. & Percy, D.M. (2015) Host-plant leaps versus host-plant shuffle: a global survey reveals contrasting patterns in an oligophagous insect group (Hemiptera, Psylloidea). *Systematics and Biodiversity*, 13 (5), 434–454. <https://doi.org/10.1080/14772000.2015.1046969>
- Ouvrard, D. (2024) Psyl'list – The World Psylloidea Database. Available from: <https://psyllist.hemiptera.infosyslab.fr/psyllist/> (accessed 1 December 2024)
- Percy, D.M. (2003) Radiation, diversity, and host-plant interactions among island and continental legume-feeding psyllids. *Evolution*, 57, 2540–2556. <https://doi.org/10.1554/02-558>
- Percy, D.M. (2017) Making the most of your host: the *Metrosideros*-feeding psyllids (Hemiptera, Psylloidea) of the Hawaiian Islands. *ZooKeys*, 649, 1–163. <https://doi.org/10.3897/zookeys.649.10213>
- Percy, D.M., Crampton-Platt, A., Sveinsson, S., Lemmon, A.R., Lemmon, E.M., Ouvrard, D. & Burckhardt, D. (2018) Resolving the psyllid tree of life: phylogenomic analyses of the superfamily Psylloidea (Hemiptera). *Systematic Entomology*, 43, 762–776. <https://doi.org/10.1111/syen.12302>
- Percy, D.M. & Cronk, Q.C. (2022) Psyllid honeydew as a *Bombus* food source in the boreal landscape. *Ecological Entomology*, 47, 713–718. <https://doi.org/10.1111/een.13147>
- Percy, D.M., Page, R.D. & Cronk, Q.C. (2004) Plant–insect interactions: double-dating associated insect and plant lineages reveals asynchronous radiations. *Systematic Biology*, 53, 120–127. <https://doi.org/10.1080/10635150490264996>
- POWO (2024) Plants of the World Online. Facilitated by the Royal Botanic Gardens, Kew. Available from: <http://www.plantsoftheworldonline.org/> (accessed 30 August 2024)
- Rübsaamen, E.H. (1908) Beiträge zur Kenntnis aussereuropäischer Zooecidien. III. Beitrag: Gallen aus Brasilien und Peru. *Marcellia*, 7, 15–79.

- Shinji, O. (1940) A new species of Japanese Psyllidae (Hemip.). *Insect World*, 44, 66–67. [in Japanese]
- Song, J., Shi, L., Li, D-Z., Sun, Y., Niu, Y., Chen, Z., Luo, H., Pang, X., Sun, Z., Liu, C., Lv, A., Deng, Y., Larson-Rabin, Z., Wilkinson, M. & Chen, S. (2012) Extensive pyrosequencing reveals frequent intra-genomic variations of internal transcribed spacer regions of nuclear ribosomal DNA. *PLoS One*, 7, e43971.
<https://doi.org/10.1371/journal.pone.0043971>
- Stamatakis, A. (2014) RAxML Version 8: A tool for phylogenetic analysis and post-analysis of large phylogenies. *Bioinformatics*, 30, 1312–1313.
<https://doi.org/10.1093/bioinformatics/btu033>
- Sun, H., Feng, J., Sun, Y., Sun, S., Li, L., Zhu, J. & Zang, H. (2023) Phytochemistry and pharmacology of *Eleutherococcus sessiliflorus* (Rupr. & Maxim.) S.Y.Hu: a review. *Molecules*, 28, 6564.
<https://doi.org/10.3390/molecules28186564>
- Swofford, D.L. (2003) *PAUP*: Phylogenetic Analysis Using Parsimony (*and Other Methods). Version 4*. Sinauer, Sunderland, Massachusetts. [program]
- Tuthill, L.D. (1944) Contributions to the knowledge of the Psyllidae of Mexico. *Journal of the Kansas Entomological Society*, 17, 143–159.
- Yang, M.M. & Raman, A. (2007) Diversity, richness, and patterns of radiation among gall-inducing psyllids (Hemiptera: Psylloidea) in the Orient and Eastern Palearctic. *Oriental Insects*, 41, 55–65.
<https://doi.org/10.1080/00305316.2007.10417499>